

Information Science Principles of Machine Learning: A Causal Chain Meta-Framework Based on Formalized Information Mapping

Jianfeng Xu

XUJF@SJTU.EDU.CN

*Koguan School of Law, China Institute for Smart Justice, School of Computer Science
Shanghai Jiao Tong University
Shanghai, 200030, China*

Editor: My editor

Abstract

This paper addresses the current lack of a unified formal framework in machine learning theory, as well as the absence of robust theoretical foundations for interpretability and ethical safety assurance. We first construct a formal information model, employing sets of well-formed formulas (WFFs) to explicitly define the ontological states and carrier mappings for the core components of machine learning. By introducing learnable and processable predicates, as well as learning and processing functions, we analyze the logical inference and constraint rules underlying causal chains in models, thereby establishing the Machine Learning Theory Meta-Framework (MLT-MF). Building upon this framework, we propose universal definitions for model interpretability and ethical safety, and rigorously prove and validate four key theorems: the equivalence between model interpretability and information existence, the constructive formulation of ethical safety assurance and two types of total variation distance (TVD) upper bounds. This work overcomes the limitations of previous fragmented approaches, providing a unified theoretical foundation from an information science perspective to systematically address the critical challenges currently facing machine learning.

Keywords: machine learning, objective information theory (OIT), formal logic systems, interpretability, ethical safety assurance, estimation of error bound

1 Introduction

Although artificial intelligence (AI), exemplified by machine learning (ML), is among the most dynamic areas in information science and technology, several critical shortcomings persist in the current research landscape. First, there is a lack of a unified logical framework that spans the entire lifecycle of machine learning. Most existing ML theory focuses on isolated components: optimization theory emphasizes training dynamics, generalization analysis targets test performance, while initialization strategies and deployment are often considered independently. This fragmentation precludes the coherent characterization of knowledge evolution from prior injection, data-driven updates, to task-level generalization (Vapnik, 1999; Alquier, 2024; Schölkopf et al., 2021; Garcez and Lamb, 2023; Marra et al., 2024).

Second, the unpredictability of model performance has led to rapidly escalating research and development costs. As model sizes continue to grow, the demands for data, computation, energy, time, and human resources have multiplied. In the absence of explicit causal semantics, structural analysis, and effective metrics, it is often challenging to analyze or predict attainable performance in each stage of the pipeline based on error upper bounds. Incomplete information coverage, suboptimal model selection, inaccurate measurement, and quality deficiencies frequently result in failed development efforts and significant resource losses (Achiam et al., 2023; Touvron et al., 2023; Chowdhery et al., 2023; Gunasekar et al., 2023).

Third, there are profound concerns regarding ethical safety assurance. As AI capabilities advance, so too do apprehensions about their ethical implications. However, there is still no consensus—either mathematical or theoretical—on the scientific definition, substantive content, forms of expression, or criteria for ethical safety in AI. Most research remains focused on ethical principles and regulatory mechanisms, while the proliferation of competing guidelines leaves practitioners uncertain about which standards to follow (Russell et al., 2015; Burr and Leslie, 2023; Tilala et al., 2024; Hawkins et al., 2021; Pant et al., 2024).

Fourth, the theoretical foundations for interpretability remain weak. The lack of a unified semantic framework for causal inference and constraint logic means that traditional ML methods treat the transformation from data to model as a black box. Although interpretability is widely recognized as a critical issue and diverse approaches have been proposed to address it, there is as yet no rigorous definition or universally applicable evaluative criteria (Lipton, 2018; Glanois et al., 2024; Zhang et al., 2024; Rudin, 2019; Miller, 2019).

As a central discipline bridging data, knowledge, and systems, information science has begun to offer new perspectives for the theoretical integration of machine learning (Shwartz-Ziv and Tishby, 2017; Xu et al., 2022). However, information science theory remains fragmented across information theory, control theory, signal processing, statistical learning, and computational theory, each developing largely in isolation and lacking a unified semantic and logical system. This fragmentation is a primary reason for the absence of a unified theoretical framework in contemporary AI. In response, Objective Information Theory (OIT) applies an axiomatic approach to construct a sextuple model of information, representing intrinsic meaning via ontological states, objective expression via carrier states, and revealing the dual-subject structure of information through the enabling mapping from the former to the latter. OIT thus provides a general and universal foundational model and metrics for understanding information in the objective world, and especially within computing and information systems (Xu et al., 2014; Xu, 2024). For example, (Xu et al., 2025) demonstrates that applying OIT’s general information metrics to pre-evaluate training data can significantly enhance model training efficiency.

This paper further defines the enabling mapping, clarifying its dual mathematical and physical-causal attributes. Through a recursively defined higher-order logical system, we formalize the expression of states via the interpretation of sets of well-formed formulas (WFFs), elucidating the mathematical essence of state representation in information definitions. This fills the final theoretical gap in OIT and offers a more powerful toolkit for applying OIT to diverse problems in information science. The introduction of noisy information and information chains further establishes the theoretical groundwork for analyzing key challenges across all stages of machine learning.

On this basis, we comprehensively apply OIT’s theories and methodologies—centered on the learnable and processable predicates, as well as learning and processing functions—to five canonical stages in machine learning: model construction, training information, learning and training, input of problems, information processing outputs and online learning. We establish a unified semantic formalization of state representation, and develop causal-chain logical inference and constraint rules covering the full ML lifecycle, culminating in the Meta-Framework for Machine Learning Theory (MLT-MF).

Applying MLT-MF, we formulate universal definitions for model interpretability and ethical safety, and prove theorems relating interpretability to information existence, as well as the theoretical underpinnings for ethical safety assurance. For model error, we establish total variation distance (TVD) upper bounds for two strategies—conservative prediction in regions not covered by training with noiseless input, and arbitrary prediction with noisy input—providing new guidelines for the estimation and optimization of machine learning performance. Finally, we illustrate and validate the practical utility of MLT-MF and the associated theorems with a simple feedforward neural network model, demonstrating that this research offers a novel direction and methodology for both theoretical analysis and engineering practice in machine learning, grounded in a unified formal logical framework.

2 Related Work

2.1 Conceptual Representations of Machine Learning

Generally, machine learning refers to methods that learn general rules from limited observational data and use these rules to predict unknown information. Numerous works have provided more detailed analyses of this concept. Representative views include:

In the context of statistical learning (Vapnik, 1999), the learning model is decomposed into three components: a set of independent random vectors x that follow a certain but unknown probability distribution $P(x)$; a set of output vectors y corresponding to input x , also following a certain but unknown conditional probability distribution $P(y|x)$; and a collection of functions $f(x, \alpha), \alpha \in \Lambda$, that the learning machine can implement. Machine learning is thus defined as selecting, based on a training dataset composed of l independent observations $(x_1, y_1), \dots, (x_l, y_l)$ drawn from the same distribution $P(x, y) = P(x)P(y|x)$, a function $f(x, \alpha)$ (with $\alpha \in \Lambda$) that minimizes the risk function $R(\alpha) = \int L(y, f(x, \alpha))dP(x, y)$, where $L(y, f(x, \alpha))$ is the loss function of $f(x, \alpha)$.

Another perspective highlights the central role of model parameters (Alquier, 2024), describing machine learning as the process of learning from an object-label set (X, Y) governed by a probability distribution P , to produce a family of predictors $\{f_\theta, \theta \in \Theta\}$ parameterized by $\theta \in \Theta$. The loss function $\uparrow(f_\theta(X), Y)$ quantifies the performance of each predictor, and the expected risk is defined as $R(\theta) = \mathbb{E}_{(X, Y) \sim P}[\uparrow(f_\theta(X), Y)]$. The ultimate goal is to find θ^* such that $R(\theta^*) = \inf_{\theta \in \Theta} R(\theta)$.

From a more advanced perspective, the focus shifts to causal relationships beyond data distribution features (Schölkopf et al., 2021). This view treats perceptual data acquired through measurement as entangled observations of unknown causal system states. It seeks to learn concrete representations that at least partially reveal these hidden causal structures by leveraging large-scale training, data augmentation, self-supervised learning, and robust fine-tuning using data from multiple simulated environments. This includes discovering

causal models implicit in environmental data and performing causal inference to plan and act based on these models.

Some researchers emphasize the integration of neural and symbolic artificial intelligence (Garcez and Lamb, 2023), arguing that knowledge should be rooted in efficient data learning via message passing in neural networks and embedded in vector representations as efficient computational models. Symbols, in turn, should be acquired through querying and extracting knowledge from trained networks, providing a rich descriptive language at appropriate levels of abstraction—allowing finite means to achieve infinite ends—while enabling compositional and discrete reasoning at the symbolic level, thereby permitting extrapolation beyond data distributions. The combination of learning and reasoning should offer an important alternative for tackling compositional reasoning problems, reducing the number of effective combinations through learning and thus generating simpler symbolic descriptions within a neuro-symbolic cycle.

Another viewpoint proposes that structure learning through parameter learning is the most prominent paradigm among the statistical relational learning approaches within neuro-symbolic AI (Marra et al., 2024). The learning task involves estimating probabilities for a fixed set of clauses, with the advantage of removing combinatorial search from the learning process.

The above works collectively reflect, from different perspectives, the academic community’s comprehensive understanding of both past achievements and future directions in machine learning. However, none have established a formalized expression for the entire lifecycle implementation process of machine learning under a unified semantic framework. As a result, it remains consistently difficult to apply structured systems analysis methods to guide the implementation and optimization of models throughout research and design.

2.2 Model Interpretability

The interpretability of machine learning has attracted significant attention in recent years. As noted in (Lipton, 2018), few authors in the academic literature are able to precisely articulate what interpretability actually means, or to clearly explain how their proposed solutions achieve it. Despite the absence of a unified definition, an increasing number of publications continue to introduce algorithms purported to possess interpretability. This situation supports two possible conclusions: first, that there is a universally accepted understanding of interpretability that simply remains unwritten; or second, that the term itself is inherently ambiguous, leading to quasi-scientific claims regarding the interpretability of various models. In reality, the objective of interpretability may simply be to extract more valuable information from models.

Reference (Glanois et al., 2024) argues that, in the context of reinforcement learning, what is considered understandable and what constitutes a good explanation may differ entirely depending on whether the end-user, system designer, or policymaker is being considered. Based on a definition of comprehensibility encompassing simulatability, decomposability, and algorithmic transparency, the authors emphasize that interpretability in reinforcement learning relies on three pillars: interpretable inputs, interpretable models, and interpretable decisions. They further analyze the specific mechanisms for achieving interpretability in each of these aspects.

In (Zhang et al., 2024), the impact of different training mechanisms on two key factors—model smoothness and gradient similarity—is investigated from the perspective of agents, with the aim of deepening our understanding of the dynamics of model transferability and its relationship to various training methods. Building on adversarial training, two working hypotheses are proposed and validated: first, that the trade-off between model smoothness and gradient similarity largely determines the adversarial transferability of agent models; and second, that shifts in data distribution can undermine gradient similarity, thereby resulting in generally poorer substitutes. This approach—explaining changes in model performance by dissecting and adjusting key factors in the training process—should be regarded as an important direction in the study of machine learning interpretability.

It is evident, therefore, that although interpretability is a critical issue in ML, the lack of a unified semantic and formal framework for machine learning has precluded the establishment of rigorous definitions and universally applicable criteria for interpretability. Approaches to enhancing interpretability remain diverse, and there is still no universally accepted methodology informed by a common theoretical foundation.

2.3 Ethical Safety Assurance

Concerns regarding the ethical safety of AI have a long history. As noted in [10], the proliferation of intelligent and autonomous systems has given rise to significant legal and moral questions, the answers to which impact both producers and consumers of AI technologies. These issues span law, public policy, professional ethics, and philosophical morality, necessitating the expertise of computer scientists, legal scholars, political scientists, and ethicists. While mathematical tools such as formal logic, probability theory, and decision theory have provided important foundations for reasoning and decision-making, numerous challenges remain unresolved.

Building on traditional concepts of assurance, [11] offers a definition of ethical assurance for AI: it is a process that employs structured argumentation to provide auditable guarantees—specifically, that a set of normative claims regarding a system’s ethical properties are justified in light of the available evidence. Accordingly, the general structure of moral assurance is characterized as an iterative process of reflection, action, and adjustment, repeated throughout the design, development, and deployment lifecycle.

In the context of AI/ML-supported healthcare, ethical safety assurance faces more concrete challenges. Reference [12] provides a comprehensive exploration of the multifaceted ethical considerations in deploying AI in healthcare. The authors advocate for multiple strategies, including the implementation of rigorous data security protocols, prioritization of data minimization, increasing diversity in training datasets, use of data augmentation to address imbalance, application of algorithmic fairness techniques to detect and mitigate model bias, regular auditing of learning algorithms, enhancing the interpretability of algorithmic outputs, regulatory oversight based on standardized performance metrics and stringent testing protocols, and the augmentation—rather than replacement—of clinicians’ capabilities as means to achieve ethical safety.

[13] further investigates safety assurance guidelines for machine learning in specific domains such as autonomous systems, establishing a causal chain from ML safety to software safety and ultimately to system safety. The authors propose that ML safety requirements

should be derived from the system-level safety requirements, and that these should be evaluated in light of the allocated safety needs, system and software architecture, and operational environment. This framework then serves as the basis for developing safety assurance specifications across all stages of the ML lifecycle, including data preparation, model training, model validation, and model deployment.

Reference [14] conducts an extensive study of the technology practitioners who have the greatest influence on AI ethical safety, proposing a classification framework that encompasses practitioner awareness, perceptions, needs, challenges, and approaches. The study highlights that, in the absence of a universally adopted set of ethical principles for AI, incorporating morality into AI is fundamentally challenged by the lack of clear moral knowledge and the ambiguity of ethical principles.

It is thus evident that, despite widespread concerns over the ethical safety of machine learning, there is as yet no mathematical or theoretical consensus regarding its scientific definition, substantive content, forms of manifestation, or criteria for assessment. Instead, ethical safety remains an open-ended concept, explored through various technical, engineering, and moral perspectives. Most research either focuses on specific ethical principles and consequences for AI, or on methods for enhancing ethical conduct. The proliferation of often conflicting AI ethical guidelines has, paradoxically, made it difficult for practitioners to determine which standards to follow. This underscores the necessity of a universally accepted definition of ethical safety, as such a definition can bridge the gap between ongoing academic discourse and industry practice, thereby providing a concrete foundation for strengthening ethical safety assurance in AI.

2.4 Model Error Estimation

Model performance is fundamentally reflected in the errors it may incur on specific tasks. Reference (Vapnik, 1999) provides key theorems on the consistency of empirical risk minimization (ERM); it characterizes the conditions for both two-sided and one-sided uniform convergence from empirical risk to true risk using VC entropy, VC dimension, and growth functions. Based on VC dimension, it further establishes distribution-independent risk upper bounds and sufficient conditions for fast convergence under both bounded and unbounded loss in finite-sample settings. By controlling the trade-off between VC dimension capacity and empirical risk through nested hypothesis families, it proves the strong consistency and convergence rates of structural risk minimization (SRM). These theoretical foundations have led to practical implementations such as support vector machines (SVM), margin maximization, and kernel methods, offering explanations for their generalization mechanisms.

Reference (Rudin, 2019) replaces global complexity with local empirical Rademacher averages, measuring complexity on subsets with small empirical error. It provides finite-sample error upper bounds via the fixed point of sub-root functions, thus achieving optimal or near-optimal convergence rates inversely proportional to the square root of the number of training samples. Under controlled variance conditions, it presents a unified framework for error estimation, including both distribution-dependent bounds determined by local Rademacher complexity and data-dependent bounds constructed from empirical local Rademacher averages. These results are extended to typical classification and regression

tasks, providing computable upper bounds and iterative algorithms for quickly approximating the fixed point.

From an information-theoretic perspective, (Miller, 2019) models learning algorithms as random channels mapping input datasets S to output hypothesis spaces W . For sub-Gaussian (including bounded) losses and uncountable hypothesis spaces, the generalization error upper bound is characterized via the mutual information $I(S; W)$ between input and output. Based on this, high-probability sample complexity and expected generalization error upper bounds are derived, and the concept of information stability (ϵ, μ) -stability is introduced, unifying algorithmic consistency and overfitting control through information leakage measures. The paper further analyzes two classes of algorithms—Gibbs learning and noisy ERM—where $I(S; W)$ is explicitly controlled via mutual information regularization, and discusses methods for decomposing and additively controlling mutual information in complex learning algorithms through adaptive combinations.

Reference (Shwartz-Ziv and Tishby, 2017) provides a foundational theoretical framework for meta-reinforcement learning, focusing on in-distribution cross-task generalization and training convergence. It introduces a task distribution T and task-level MDPs, defines generalization error as the performance gap between training and unseen tasks under a meta-policy, and establishes generalization upper bounds determined by the number of training tasks and task complexity, using empirical process theory and concentration inequalities. The analysis further discusses the impact of algorithmic capacity and learning rates on error bounds. Within the non-convex SGD framework, sufficient conditions and rates for finite-step convergence of meta-learning loss are presented, along with guidelines for long-term behavior and hyperparameter selection based on linear and sub-linear types. The theoretical results are validated and the observability of convergence rates is demonstrated through controllable task generation and baseline meta-algorithms.

Reference (Xu et al., 2022) addresses the separation and convergence complexity of continuous and discrete errors in deterministic sampling of generative models. From both theoretical and numerical perspectives, it investigates the convergence properties of deterministic samplers based on probability flow ordinary differential equations (ODEs). Assuming access to score function estimates with L_2 accuracy, it provides upper bounds on TVD between target and generated distributions in continuous time. For the practical implementation using Runge-Kutta integrators, discrete-time error upper bounds are established. Numerical experiments on 128-dimensional problems are conducted to validate these theoretical error bounds.

Collectively, these works encompass both classical statistical learning theory and recent advances in reinforcement learning and generative models, reflecting a broad recognition of the importance of model error upper bounds in machine learning. However, these studies do not employ explicit causal semantic modeling, nor do they address the full lifecycle challenges of multi-stage information transmission, online learning, or multi-agent integration in ML. Additionally, they rarely consider the geometric scale and entropy of distribution shifts and uncovered domains, making it difficult to offer actionable engineering or data-sampling guidance for test domain coverage gaps and noisy input scenarios.

3 Preliminary Theory

Undoubtedly, as a key component of artificial intelligence, modern machine learning is a product of the rapid development and high integration of information technologies such as computers, the Internet, big data, and cloud computing. Machine learning systems are, without question, an important branch of information systems. Starting from the basic concept of information can provide a unified theoretical foundation for research in machine learning and artificial intelligence.

3.1 Definition of Information

Reference (Xu et al., 2014), based on four fundamental postulates, proposes that information is an enabling mapping from the state of an ontology to the state of a carrier, but does not further elaborate on the notions of “state” or “enabling mapping.” Appendix A establishes a higher-order formal system \mathcal{L} and, drawing on general common sense, formulates basic postulates regarding states. It is then proven that any set of states can be represented as the interpretation of a set of WFFs in \mathcal{L} (Xu, 2024), indicating that both ontological states and carrier states correspond to interpretations of sets of WFFs over specific domains of objects and times. Here, we proceed to further clarify the concept of enabling mapping.

Definition 1 (Enabling Mapping) Let X and Y be two sets, and let f be a mapping. If for any $x \in X$, there exists a $y \in Y$, and for any $y \in Y$, there exists at least one $x \in X$ such that $y = f(x)$, and furthermore, the existence of y is physically realized only because of x , then f is called an enabling mapping from X to Y . This is denoted as:

$$f : X \rightrightarrows Y \tag{3.1}$$

or

$$f(X) \supseteq Y \tag{3.2}$$

In (3.1) and (3.2), the symbols \rightrightarrows and \supseteq are used to indicate enabling mappings, which differ from the standard notation \rightarrow and $=$ used for ordinary mappings. This distinction signifies that X not only establishes a surjective mapping with Y in the mathematical sense, but also forms a physical causal enabling relationship between the two. It is thus evident that every element of Y is induced by X , and therefore, the enabling mapping f must be surjective. To simplify the discussion, unless otherwise specified, we assume in the following that f is single-valued. Accordingly,

Corollary 1 If f is an enabled mapping from X to Y , then $|X| \geq |Y|$, where $|X|$ and $|Y|$ denote the cardinalities of the sets X and Y , respectively.

If $f(X) \supseteq Y$, we also denote this as $f^{-1}(y) \triangleleft x$ or $x \triangleright f^{-1}(y)$, to maintain consistency in the directionality of enabling. Fig.1(a) intuitively illustrates the dual nature of an enabling mapping, encompassing both its mathematical mapping and physical enabling attributes.

Based on this, a more rigorous theoretical foundation for the definition of information can be established:

Definition 2 (Mathematical Definition of Information) Let \mathbb{O} denote the set of objective entities, \mathbb{S} the set of subjective entities, and \mathbb{T} the set of times, with elements of \mathbb{O} , \mathbb{S} , and \mathbb{T} partitioned as needed depending on the domain. The ontology $o \subseteq \mathbb{O} \cup \mathbb{S}$, time of

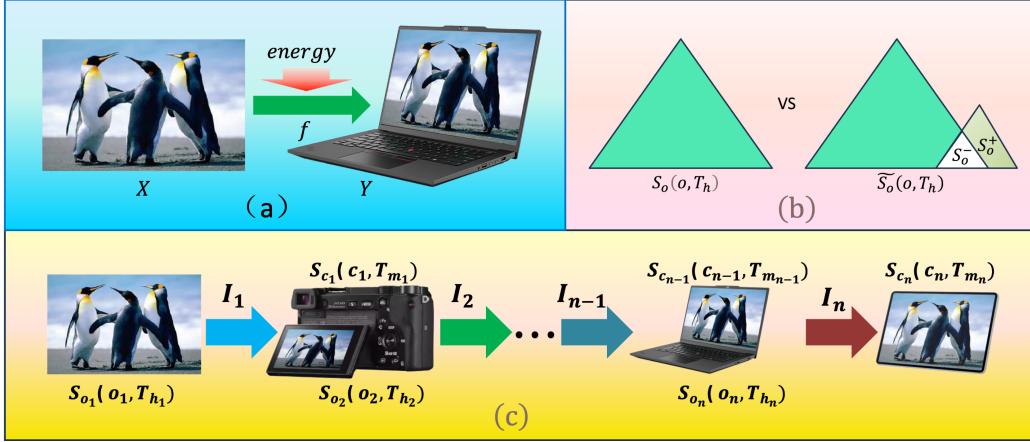


Figure 1: Schematic Diagram of Enabling Mapping, Noisy Information, and Information Transmission Chain. (a) The scene of penguin activity X is mapped by an enabling mapping f to an image Y on a laptop; between X and Y there exists both a mathematical mapping relationship and a causal relationship. Moreover, mapping X to Y requires corresponding physical conditions and the expenditure of a certain amount of energy. (b) The left panel depicts the ontological state of noiseless information, while the right panel shows a noisy information state: the set S_o^- is removed from the noiseless ontological state, and the previously disjoint set S_o^+ is superimposed, resulting in a noisy ontological state. (c) In the penguin activity information transmission chain, the carrier state of any subsequent piece of information can be regarded as the result of an enabling mapping from any prior ontological information state, and can also be reasonably interpreted by means of this ontological state and the corresponding enabling mapping.

occurrence $T_h \subseteq \mathbb{T}$, ontological state set $S_o(o, T_h)$, carrier $c \subseteq \mathbb{O}$, reflection time $T_m \subseteq \mathbb{T}$, and carrier reflection set $S_c(c, T_m)$ are all non-empty sets. Then, information I is the enabling mapping from $S_o(o, T_h)$ to $S_c(c, T_m)$, succinctly denoted as $I = \langle o, T_h, S_c, c, T_m, S_o \rangle$. The set of all information I is called the information space, denoted by \mathfrak{I} , which, together with matter and energy, forms the three fundamental constituents of the objective world (Xu et al., 2025).

It should be noted that both $S_o(o, T_h)$ and $S_c(c, T_m)$ can each be represented as the interpretation of a set of WFFs within a formal system. However, the respective formal systems need not be identical, which constitutes one of the essential characteristics of information—its capacity to establish connections among all entities in the world, regardless of differences in their underlying formal systems.

Reference (Shannon, 1948) is regarded as a foundational work in information theory. The paper proposed that " $H = -\sum p_i \log p_i$ plays a central role as the measure of information in information theory." The discussion in this paper includes both the source and channel of information. The source I_s is the origin of the information, and it generates events e_1, e_2, \dots, e_n with probabilities p_1, p_2, \dots, p_n , respectively. The channel I_c is the medium

through which information is transmitted. After an event e_i occurs at time T_h in the source Is , the channel Ic receives and transmits the corresponding code c_i in the time interval $(T_h, T_h + \tau)$ (where $1 \leq i \leq n$, $\tau > 0$). We define the ternary predicate $IsEvent^3(Is, T_h, e_i)$ to represent that event e_i happened in source Is at time T_h , and the ternary predicate $IcCode^3(Ic, T_m, c_i)$ to represent that the channel Ic received and transmitted code c_i in the time interval T_m . Then,

$$S_{Is}(Is, T_h) = IsEvent^3(Is, T_h, e_i) \quad (3.3)$$

and

$$S_{Ic}(Ic, (T_h, T_h + \tau)) = IcCode^3(Ic, (T_h, T_h + \tau), c_i) \quad (3.4)$$

are the states of the source Is at time T_h and the state of the channel Ic in the time interval $(T_h, T_h + \tau)$, respectively (where $1 \leq i \leq n$). Furthermore,

$$I : S_{Is}(Is, T_h) \Rightarrow S_{Ic}(Ic, (T_h, T_h + \tau)) \quad (3.5)$$

represents the enabling mapping from the source state $S_{Is}(Is, T_h)$ to the channel state $S_{Ic}(Ic, (T_h, T_h + \tau))$. Therefore, although Shannon's information theory investigates the various probability distributions of $S_{Is}(Is, T_h)$ and the complex implementation mechanisms of $S_{Ic}(Ic, (T_h, T_h + \tau))$, it forms a rich and extensive theoretical system. The OIT definition of information can encompass Shannon's most original model of information, indicating that it has a broader and more universal application range.

3.2 Noisy Information

The realization of information is often influenced by noise or other external factors. Therefore, the following concept is introduced:

Definition 3 (Noisy Information) For information $I = \langle o, T_h, S_o, c, T_m, S_c \rangle$, let $\widetilde{S}_o(o, T_h)$ be another state of the ontology o at time T_h , and $\widetilde{S}_c(c, T_m)$ be another state of the carrier c at time T_m ,

$$\widetilde{S}_o(o, T_h) = S_o(o, T_h) \setminus S_o^-(o, T_h) \cup S_o^+(o, T_h) \quad (3.6)$$

where the state $S_o^-(o, T_h)$ is the loss state of $S_o(o, T_h)$, satisfying $S_o^-(o, T_h) \subseteq S_o(o, T_h)$ and not being enabled to map to $\widetilde{S}_c(c, T_m)$, and the state $S_o^+(o, T_h)$ is the superposed state of $S_o(o, T_h)$, satisfying $S_o(o, T_h) \cap S_o^+(o, T_h) = \emptyset$ and being enabled to map to $\widetilde{S}_c(c, T_m)$. The enabling mapping is then defined as:

$$\widetilde{I} : \widetilde{S}_o(o, T_h) \Rightarrow \widetilde{S}_c(c, T_m) \quad (3.7)$$

which is the noisy information of I , while I is its own noiseless information. Thus, the noisy information \widetilde{I} is also information. It has the same ontology, time of occurrence, carrier, and reflection time as I , but the states of the entity and carrier may overlap but are not completely the same. Fig.1(b) illustrates the structural characteristics of noisy information.

In fact, Shannon also started by discussing the ideal noiseless channel and then discussed the more complicated noisy channel scenario (Shannon, 1948). In this case, he assumes that the signal generated by the source is S , the channel noise is N , and the channel output is:

$$E = f(S, N) \quad (3.8)$$

where f is the distortion function of the channel to the transmitted signal. According to OIT's view, the signal S here is the ontological state of information I , $S_{I_s}(I_s, T_h)$. The distortion function $f(S, N)$ for signal S and noise N is equivalent to removing a state $S_{I_s}^-(I_s, T_h)$ from the source state $S_{I_s}(I_s, T_h)$ and adding another state $S_{I_s}^+(I_s, T_h)$. The output E is then the channel's output state $\widetilde{S}_{I_c}(I_c, (T_h, T_h + \tau))$, where $(T_h, T_h + \tau)$ is the time interval of the channel output. Thus,

$$\widetilde{I} : \widetilde{S}_{I_s}(I_s, T_h) \Rightarrow \widetilde{S}_{I_c}(I_c, (T_h, T_h + \tau)) \quad (3.9)$$

is the noisy information of

$$I : S_{I_s}(I_s, T_h) \Rightarrow S_{I_c}(I_c, (T_h, T_h + \tau)) \quad (3.10)$$

where $\widetilde{S}_{I_s}(I_s, T_h) = S_{I_s}(I_s, T_h) \setminus S_{I_s}^-(I_s, T_h) \cup S_{I_s}^+(I_s, T_h)$.

In this way, we use the definition of noisy information to explain Shannon's model of noisy channels in (Shannon, 1948), demonstrating that OIT is applicable to the complex scenarios of information research under noisy conditions.

3.3 Information Chain

Reference (Xu et al., 2014) discusses the transmissibility of information through composite mappings. Based on Definitions 1 and 2, the fundamental laws governing information transmission can be characterized more rigorously as follows:

Lemma 1 (Transmissibility of Information): Let $I_0 = \langle o, T_h, S_o, c_1, T_{m_1}, S_{c_1} \rangle$ and $I_1 = \langle c_1, T_{m_1}, S_{c_1}, c_2, T_{m_2}, S_{c_2} \rangle$ be two pieces of information. Then, $I_2 = \langle o, T_h, S_o, c_2, T_{m_2}, S_{c_2} \rangle$ is also information. We refer to this as the information I_0 being transmitted from carrier c_1 to carrier c_2 via c_1 .

Proof: According to Definitions 1 and 2, as well as the given conditions, for any $S_o(x, t) \in S_o(o, T_h)$, there exists $S_{c_1}(x_1, t_1) \in S_{c_1}(c_1, T_{m_1})$ such that $I_0(S_o(x, t)) \supseteq S_{c_1}(x_1, t_1)$. Furthermore, there exists $S_{c_2}(x_2, t_2) \in S_{c_2}(c_2, T_{m_2})$ such that $I_1(S_{c_1}(x_1, t_1)) \supseteq S_{c_2}(x_2, t_2)$. Define $I_2(S_o(x, t)) = S_{c_2}(x_2, t_2)$. Since the physical realization of $S_{c_2}(x_2, t_2)$ is contingent upon the existence of $S_{c_1}(x_1, t_1)$, and the physical realization of $S_{c_1}(x_1, t_1)$ in turn depends on $S_o(x, t)$, by causal induction, the physical realization of $S_{c_2}(x_2, t_2)$ ultimately depends on $S_o(x, t)$.

Conversely, for any $S_{c_2}(x_2, t_2) \in S_{c_2}(c_2, T_{m_2})$, there exists $S_{c_1}(x_1, t_1) \in S_{c_1}(c_1, T_{m_1})$ such that $I_1(S_{c_1}(x_1, t_1)) \supseteq S_{c_2}(x_2, t_2)$; and there also exists $S_o(x, t) \in S_o(o, T_h)$ such that $I_0(S_o(x, t)) \supseteq S_{c_1}(x_1, t_1)$. Thus, $I_2(S_o(x, t)) = I_1(I_0(S_o(x, t))) \supseteq I_1(S_{c_1}(x_1, t_1)) \supseteq S_{c_2}(x_2, t_2)$.

Therefore, $I_2 = \langle o, T_h, S_o, c_2, T_{m_2}, S_{c_2} \rangle$ is an enabling mapping from $S_o(o, T_h)$ to $S_{c_2}(c_2, T_{m_2})$, which satisfies the definition of information as given in Definition 2. In essence, this is the information I_0 transmitted from carrier c_1 to carrier c_2 . The lemma is thus proved.

Corollary 2 (Information Chain) Let $\{I_i = \langle o_i, T_{h_i}, S_{o_i}, c_i, T_{m_i}, S_{c_i} \rangle | i = 1, \dots, n\}$ be a sequence of information mappings, where for any $i > 1$, it holds that $o_i = c_{i-1}, T_{h_i} =$

$T_{m_{i-1}}$, and $S_{o_i}(o_i, T_{h_i}) = S_{c_{i-1}}(c_{i-1}, T_{m_{i-1}})$. In this case, we say that these mappings constitute an information chain. Moreover, for any $1 \leq i \leq j \leq n$, $I_{ij} = \langle o_i, T_{h_i}, S_{o_i}, c_j, T_{m_j}, S_{c_j} \rangle$ also qualifies as information according to Definition 2.

Transmission constitutes a fundamental mode of information flow and application. Communication, processing, input, and output are all concrete realizations of information transmission. In many cases, information undergoes more complex flows through chain-like transmission processes. Fig.1(c) intuitively illustrates such a process. For any pair of states within this process, the latter can be regarded as the result of the enabling mapping from the former, and this enabling mapping can be used to reasonably explain the causation of the latter state. This provides a theoretical foundation for the interpretability of the model.

4 Meta-Framework for Machine Learning Theory (MLT-MF)

The core of machine learning is the artificial intelligence model, which can be regarded as a finite automaton as well as an information system. The processes of operation, learning, testing, and application for such a model all fundamentally depend on information within the system. Therefore, by employing the concepts of information model and finite automaton state (Appendix B), the process of machine learning and its applications can be unified into five primary steps of information realization and functioning:

4.1 Construction of Initial Information

Suppose the model under study is denoted as M , and let $T = \{t_i | i = 1, \dots, n\}$ be the set of time points at which M , as a finite automaton, undergoes assignment, input, output, and state transitions in increasing order. According to the perspective of OIT, the creation of M is essentially the realization of information

$$I_o = \langle M_D, T_{o_h}, S_{M_D}, M, t_1, S_M \rangle \quad (4.1)$$

where the ontology M_D of I_o is the designer's conceptualization of M , T_{o_h} is the time at which the designer conceives M , and $S_{M_D}(M_D, T_{o_h})$ is the initial finite automaton state that must be realized at this conceptual stage. The carrier M of I_o is the model itself; the reflection time t_1 is when M is constructed according to $S_{M_D}(M_D, T_{o_h})$; and $S_M(M, t_1)$ is the formalization of the actual physical state of M upon its completion. Thus, $\text{sup}(T_{o_h}) < \text{sup}(t_1)$.

According to Lemma B.2, let the binary function $\Phi^2(X, t)$ represent the set of structures, parameters, and algorithms of model X at time t . The formula

$$\varphi_{o_1} = \text{State}^3(M_D, t_1, \Phi^2(M_D, T_{o_h})) \quad (4.2)$$

denotes that, at time t_1 , the initial structure, parameters, and algorithm set $\Phi^2(M_D, T_{o_h})$ as envisioned by the designer are assigned to M_D .

$$\begin{aligned} \varphi_{o_2} = & \text{State}^3(M_D, t_1, \Phi^2(M_D, T_{o_h})) \wedge \text{Input}^3(M_D, t_1, S_{M_I}(M_I, t_1)) \\ & \wedge \text{Learnable}^2(M_D, S_{M_I}(M_I, t_1)) \rightarrow \exists f_{\text{learn}}^2(M_D, S_{M_I}(M_I, t_1)) \\ & (\text{Eq}^2(\Phi^2(M_D, t_2), f_{\text{learn}}^2(M_D, S_{M_I}(M_I, t_1)))) \wedge \text{State}^3(M_D, t_2, \Phi^2(M_D, t_2)) \end{aligned} \quad (4.3)$$

expresses that, at time t_1 , when the structure, parameters, and algorithm set of M_D is $\Phi^2(M_D, T_{oh})$, and the input carrier state $S_{M_I}(M_I, t_1)$ is provided and satisfies the learnability condition determined by the binary predicate $Learnable^2(M_D, S_{M_I}(M_I, t_1))$, M_D can optimize its internal structures, parameters, and algorithms to $\Phi^2(M_D, t_2)$ through the learning binary function $f_{learn}^2(M_D, S_{M_I}(M_I, t_1))$, assigning this to M_D . This demonstrates the model's capacity for learning and optimization, where M_I denotes the input device of M .

$$\begin{aligned} \varphi_{o_3} = & State^3(M_D, t_1, \Phi^2(M_D, T_{oh})) \wedge Input^3(M_D, t_1, S_{M_I}(M_I, t_1)) \\ & \wedge Processable^2(M, S_{M_I}(M_I, t_1)) \rightarrow \exists f_{process}^2(M, S_{M_I}(M_I, t_1)) \\ & (Eq^2(S_{M_O}(M_O, t_2), f_{process}^2(M, S_{M_I}(M_I, t_1))) \wedge Output^3(M, t_2, S_{M_O}(M_O, t_2))) \end{aligned} \quad (4.4)$$

indicates that, at time t_1 , if $S_{M_I}(M_I, t_1)$ is input into M_D and meets the processability condition specified by the binary predicate $Processable^2(M, S_{M_I}(M_I, t_1))$, then M_D can process $S_{M_I}(M_I, t_1)$ via the binary processing function $f_{process}^2(M, S_{M_I}(M_I, t_1))$ to yield the output carrier state $S_{M_O}(M_O, t_2)$, which is then output at time t_2 . This demonstrates the model's ability to process and output information, where M_O denotes the output device of M .

Thus,

$$S_{M_D}(M_D, T_{oh}) = \{\varphi_{o_1}, \varphi_{o_2}, \varphi_{o_3}\} \quad (4.5)$$

constitutes the initial state of M as conceived by the designer.

It should be noted that, since M_D , $\Phi^2(M_D, T_{oh})$, and $State^3(M_D, t_1, \Phi^2(M_D, T_{oh}))$ all represent sets, $\varphi_{o_1}, \varphi_{o_2}, \varphi_{o_3}$ may be considered as three well-formed formulas, or—when decomposed with respect to the elements of each set—as three sets of more granular well-formed formulas. Regardless of the situation, both cases satisfy Definition 4 concerning finite automaton states. Therefore, subsequent discussions will encompass both cases without further elaboration.

$S_{M_D}(M_D, T_{oh})$ may represent the designer's idea, a design draft on paper, or an electronic document. Through the information Io , these are enabled and mapped into the physically operational state of the model M :

$$S_M(M, t_1) = \{\psi_{o_1}, \psi_{o_2}, \psi_{o_3}\} \quad (4.6)$$

where $\psi_{o_1} \triangleq Io(\varphi_{o_1})$, $\psi_{o_2} \triangleq Io(\varphi_{o_2})$, and $\psi_{o_3} \triangleq Io(\varphi_{o_3})$ are the enabling mappings of $\varphi_{o_1}, \varphi_{o_2}, \varphi_{o_3}$, respectively. This process establishes M as a typical finite automaton and an operational information system.

4.2 Formal Modeling and Realization of Training Information

According to the general formal definition of information, the formal expression for the realization of training information is straightforward:

$$It = \langle ot, Tt_h, S_{ot}, M_I, t_1, S_{M_I} \rangle \quad (4.7)$$

$$S_{ot}(ot, Tt_h) = \{\varphi t | \varphi t \text{ is a WFF about } ot \text{ and } Tt_h\} \quad (4.8)$$

$$S_{M_I}(M_I, t_1) = \{\psi t | \psi t \text{ is a WFF about } M_i \text{ and } t_1\} \quad (4.9)$$

Here, the ontology ot refers to the object containing knowledge or samples; Tt_h is the time at which its state is formed; and $S_{ot}(ot, Tt_h)$ is a set of business-oriented semantic assertions or facts about the ontology. M_I functions similarly to the hardware interface and API software of M , carrying the training information at time t_1 . The carrier state $S_{M_I}(M_I, t_1)$ is the physical realization of $S_{ot}(ot, Tt_h)$ via an enabling mapping, ensuring that the information can be machine-read and entered into M .

4.3 Formal Modeling and Implementation of Model Learning

Model learning for M involves fusing its original information Io with the training information It , resulting in updated information:

$$Iu = \langle M \cup M_I, t_1 \cup t_2, S_{M \cup M_I}, M, t_2, S_M \rangle \quad (4.10)$$

Here, the ontology is the hybrid $M \cup M_I$, encompassing both the model and its interface; $t_1 \cup t_2$ marks the time of the first learning event; and $S_{M \cup M_I}(M \cup M_I, t_1 \cup t_2)$ formally represents the hybrid state during learning:

$$S_{M \cup M_I}(M \cup M_I, t_1 \cup t_2) = \{\varphi u_1, \varphi u_2, \varphi u_3\} \quad (4.11)$$

$$\varphi u_1 = Eq^2(\Phi^2(M, t_2), f_{learn}^2(M, S_{M_I}(M_I, t_1))) \wedge State^3(M, t_2, \Phi^2(M, t_2)) \quad (4.12)$$

indicates that the input state $S_{M_I}(M_I, t_1)$, which was learned by M at time t_1 , has been transformed into a new set of structures, parameters, and algorithms $\Phi^2(M, t_2)$ at time t_2 , thus becoming the state of M at t_2 .

$$\begin{aligned} \varphi u_2 = & State^3(M, t_2, \Phi^2(M, t_2)) \wedge Input^3(M, t_2, S_{M_I}(M_I, t_2)) \\ & \wedge Learnable^2(M, S_{M_I}(M_I, t_2)) \rightarrow \exists f_{learn}^2(M, S_{M_I}(M_I, t_2)) \\ & (Eq^2(\Phi^2(M, t_3), f_{learn}^2(M, S_{M_I}(M_I, t_2)))) \wedge State^3(M, t_3, \Phi^2(M, t_3)) \end{aligned} \quad (4.13)$$

shows that after the first learning step, M remains capable of further learning and optimization.

$$\begin{aligned} \varphi u_3 = & State^3(M, t_2, \Phi^2(M, t_2)) \wedge Input^3(M, t_2, S_{M_I}(M_I, t_2)) \\ & \wedge Processable^2(M, S_{M_I}(M_I, t_2)) \rightarrow \exists f_{process}^2(M, S_{M_I}(M_I, t_2)) \\ & (Eq^2(S_{M_O}(M_O, t_3), f_{process}^2(M, S_{M_I}(M_I, t_2)))) \wedge Output^3(M, t_3, S_{M_O}(M_O, t_3)) \end{aligned} \quad (4.14)$$

indicates that when the training information It is processable by M , it can also produce output information.

This state is then enabled and mapped to the physical state of the carrier M at time t_2 :

$$S_M(M, t_2) = \{\psi u_1, \psi u_2, \psi u_3\} \quad (4.15)$$

4.4 User Input Information for the Model

User input information is formally given by:

$$Iq = \langle oq, Tq_h, S_{oq}, M_I, t_2, S_{M_I} \rangle \quad (4.16)$$

$$S_{oq}(oq, Tq_h) = \{\varphi q | \varphi q \text{ is a WFF about } oq \text{ and } Tq_h\} \quad (4.17)$$

$$S_{M_I}(M_I, t_2) = \{\psi q | \psi q \text{ is a WFF about } M_I \text{ and } t_2\} \quad (4.18)$$

Here, the ontology oq represents the user's intention or device, with Tq_h denoting the time at which the ontological state is formed. The state $S_{oq}(oq, Tq_h)$ is the formal representation of the user's needs. The carrier state $S_{M_I}(M_I, t_2)$ is the physical realization, via enabling mapping, of $S_{oq}(oq, Tq_h)$ onto the model's interface device M_I .

4.5 Information Processing, Output, and Online Learning of the Model

When the model M processes input and produces output, the information it carries can be represented as:

$$Iv = \langle M \cup M_I \cup M_O, t_2 \cup t_3, S_{M \cup M_I \cup M_O}, M, t_3, S_M \rangle \quad (4.19)$$

where:

$$S_{M \cup M_I \cup M_O}(M \cup M_I \cup M_O, t_2 \cup t_3) = \{\varphi v_1, \varphi v_2, \varphi v_3\} \quad (4.20)$$

$$\varphi v_1 = State^3(M, t_2, \Phi^2(M, t_2)) \quad (4.21)$$

indicates that $\Phi^2(M, t_2)$ has been assigned to M at time t_2 .

$$\begin{aligned} \varphi v_2 = & Input^3(M, t_2, S_{M_I}(M_I, t_2)) \wedge Eq^2(S_{M_O}(M_O, t_3), f_{process}^2(M, S_{M_I}(M_I, t_2))) \\ & \wedge Output^3(M, t_3, S_{M_O}(M_O, t_3)) \end{aligned} \quad (4.22)$$

indicates that when the input state $S_{M_I}(M_I, t_2)$ is received at t_2 , M produces the output state $S_{M_O}(M_O, t_3)$ at t_3 .

$$\begin{aligned} \varphi v_3 = & State^3(M, t_2, \Phi^2(M, t_2)) \wedge Input^3(M, t_2, S_{M_I}(M_I, t_2)) \wedge Learnable^2(M, S_{M_I}(M_I, t_2)) \\ & \rightarrow \exists f_{learn}^2(M, S_{M_I}(M_I, t_2))(Eq^2(\Phi^2(M, t_3), f_{learn}^2(M, S_{M_I}(M_I, t_2)))) \\ & \wedge State^3(M, t_3, \Phi^2(M, t_3)) \end{aligned} \quad (4.23)$$

expresses that if the input information can be learned by M , then M can achieve online learning while processing and outputting information.

The physical realization of this state through an enabling mapping is:

$$S_M(M, t_3) = \{\psi v_1, \psi v_2, \psi v_3\} \quad (4.24)$$

The output information is given by:

$$Ir = \langle M \cup M_I, t_2, S_{M \cup M_I}, M_O, t_3, S_{M_O} \rangle \quad (4.25)$$

where the ontological state is:

$$S_{M \cup M_I}(M \cup M_I, t_2) = \{\varphi r_1\} \quad (4.26)$$

with

$$\varphi r_1 = Eq^2(S_{M_O}(M_O, t_3), f_{process}^2(M, S_{M_I}(M_I, t_2))) \quad (4.27)$$

The formal expression of the physical state of the model's output device M_O at time t_3 is:

$$S_{M_O}(M_O, t_3) = \{\psi r_1\} \quad (4.28)$$

The model can repeat the processes described in Sections 3.2 to 3.5, iterating through cycles of training and information processes to meet user demands and continuously improve its performance.

4.6 Multi-Stage Information Causal Chains

From systems engineering perspective, the realization of information in machine learning involves more than just five information mappings. In practice, stages such as requirements analysis, design and development, and system integration are also necessary. Specifically, in the four stages of model construction, learning and training, problem input, and answer output, and according to the corollary on information chains in Section 3.3, there is a causal and progressive process that moves from conceptual ideas to mind maps, program code, and finally to physical implementation. In this process, the earlier content serves as the ontological state, while the subsequent content becomes the carrier state, sequentially forming conceptual information, design information, and implementation information (see Fig.2).

Fig.2 presents a comprehensive framework of formal expressions and causal information progression for each stage of the machine learning process, from the perspectives of OIT and finite automaton state implementation. This framework transcends specific algorithms or models, offering a novel, unified, and general framework—MLT-MF—for addressing several key issues in the field of machine learning. In Appendix C, we further provide an example of its application to feedforward neural networks, thereby testing the correctness and applicability of the framework and supporting the verification of related theorems.

In machine learning, the four distinct stages—model construction, learning and training, problem input, and answer output—each encompass four levels: conceptual ideas, mind

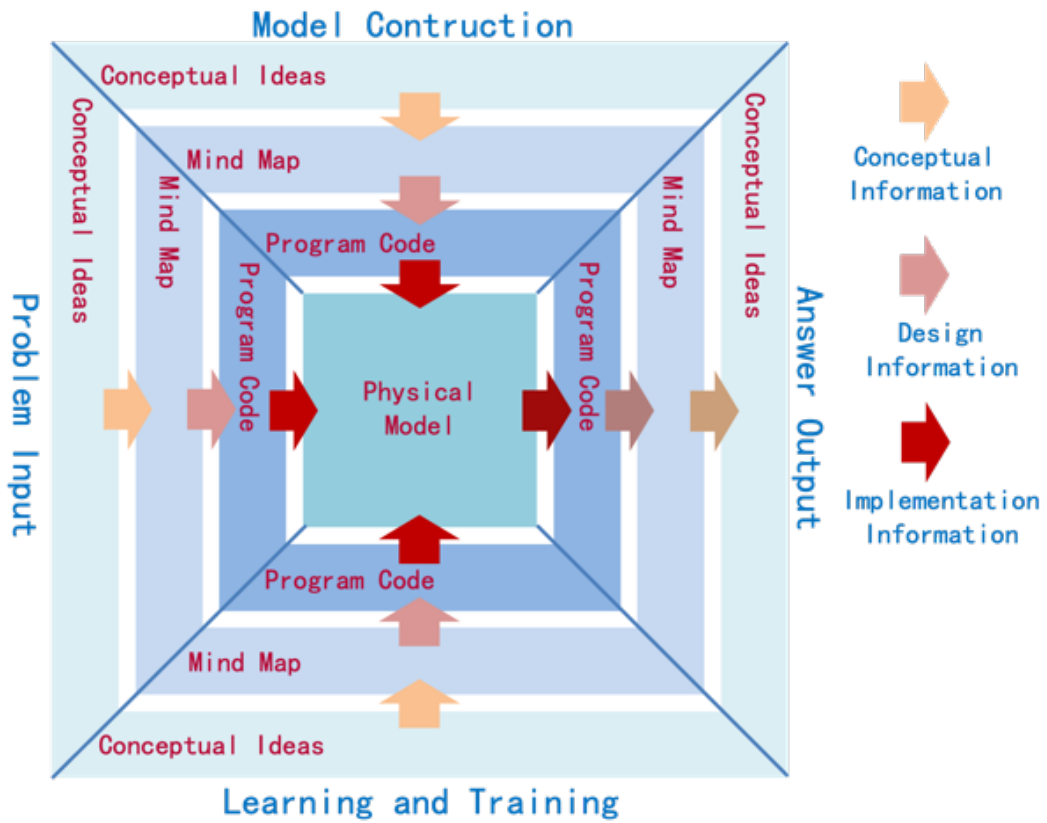


Figure 2: Causal Chains of Multiple Information Mappings in Machine Learning.

maps, program code, and physical models. Generally, the content within the same level shares a common semantic logic and can thus be represented using a unified formal system. Furthermore, owing to the transmissibility of information, the innermost physical model can be regarded as the result of an enabling mapping from the outer conceptual ideas or mind maps. The output stage can, in turn, be viewed as a reverse causal transmission from the physical model back to conceptual ideas. This demonstrates that the system comprises multiple stages, with each stage containing various combinatorial information causal chains.

5 Several Important Definitions and Theorems

The MLT-MF framework is applicable to a range of key issues in the field of artificial intelligence, offering many unique and practical theoretical principles and methodological guidelines.

5.1 Theorem of Model Interpretability

According to the view that interpretability should be a concept dependent on the domain of discourse and the corresponding logical system, and that interpretability should also be related to the specific inputs and outputs of the model (Glanois et al., 2024), the following concepts are established based on the MLT-MF framework:

Definition 4 (Model Interpretability) Let the model M , as a finite automaton, operate over an ordered set of times $T = \{t_i | i = 1, \dots, n\}$, at which it undergoes assignment, input, output, and state transitions. The state of M at time t_i is denoted as $S_M(M, t_i)$, and the state of its input device M_I at time t_i is $S_{M_I}(M_I, t_i)$, while the state of the output device M_O at time t_{i+1} is $S_{M_O}(M_O, t_{i+1})$. If there exists a formal system \mathcal{L} along with three interpretations E_M , E_{M_I} , and E_{M_O} over the finite domains D_M , D_{M_I} , and D_{M_O} respectively, such that

$$E_{M_O} \subseteq Cn(E_M \cup E_{M_I}) \quad (5.1)$$

making $S_M(M, t_i)$, $S_{M_I}(M_I, t_i)$, and $S_{M_O}(M_O, t_{i+1})$ the respective enabling mappings of E_M , E_{M_I} , and E_{M_O} , then M is said to be interpretable in \mathcal{L} with respect to output $S_{M_O}(M_O, t_{i+1})$ under input $S_{M_I}(M_I, t_i)$. If for all $i = 1, \dots, n - 1$, the output $S_{M_O}(M_O, t_{i+1})$ under input $S_{M_I}(M_I, t_i)$ is interpretable in \mathcal{L} , then M is called interpretable in \mathcal{L} .

Here, $Cn(E_M \cup E_{M_I})$ denotes the logical closure of $E_M \cup E_{M_I}$. Equation (5.1) states that in the formal system \mathcal{L} , all formulas in E_{M_O} are logical consequences of E_M and E_{M_I} . Moreover, since $S_M(M, t_i)$, $S_{M_I}(M_I, t_i)$, and $S_{M_O}(M_O, t_{i+1})$ are respectively enabled by E_M , E_{M_I} , and E_{M_O} , the formal system \mathcal{L} and its three interpretations fully capture the logical and causal relationship whereby M produces output $S_{M_O}(M_O, t_{i+1})$ under input $S_{M_I}(M_I, t_i)$. This, in essence, offers a concise understanding of model interpretability.

Theorem 1 (Model Interpretability and Information Existence) Let the model M be viewed as a finite automaton operating over an ordered set of times $T = \{t_i | i = 1, \dots, n\}$, during which it undergoes assignment, input, output, and state transitions.

(1) For any $1 \leq i \leq n - 1$, a necessary and sufficient condition for the output $S_{M_O}(M_O, t_{i+1})$ of model M to be interpretable in the formal system \mathcal{L} under the input $S_{M_I}(M_I, t_i)$ is that

there exist $Iu(t_i) = \langle ou(t_i), Tu_h(t_i), Sou, M, t_i, S_M \rangle$ and $Iq(t_i) = \langle oq(t_i), Tq_h(t_i), Soq, M_I, t_i, S_{M_I} \rangle$ representing the information carried by M and its input device M_I at time t_i , respectively, and $Ir(t_{i+1}) = \langle or(t_{i+1}), Tr_h(t_{i+1}), Sor, M_O, t_{i+1}, S_{M_O} \rangle$ representing the information carried by the output device M_O at time t_{i+1} . The ontological states of these three pieces of information must each correspond to an interpretation in \mathcal{L} , and $S_{or}(or(t_{i+1}), Tr_h(t_{i+1})) \subseteq Cn(S_{ou}(ou(t_i), Tu_h(t_i)) \cup S_{oq}(oq(t_i), Tq_h(t_i)))$ must hold.

(2) A necessary and sufficient condition for M to be interpretable in \mathcal{L} is that, for all $i = 1, \dots, n-1$, there exist information objects $Iu(t_i)$, $Iq(t_i)$, and $Ir(t_{i+1})$ whose ontological states are all interpretations in \mathcal{L} , and such that the ontological state of $Ir(t_{i+1})$ is contained in the logical closure of the union of the ontological states of $Iu(t_i)$ and $Iq(t_i)$.

Proof: For any $1 \leq i \leq n-1$, suppose that the output $S_{M_O}(M_O, t_{i+1})$ of model M under the input $S_{M_I}(M_I, t_i)$ is interpretable in the formal system \mathcal{L} . According to Definition 4, there exist three interpretations E_M , E_{M_I} , and E_{M_O} in the formal system \mathcal{L} , respectively over the finite domains D_M , D_{M_I} , and D_{M_O} , such that $E_{M_O} \subseteq Cn(E_M \cup E_{M_I})$, and $S_M(M, t_i)$, $S_{M_I}(M_I, t_i)$, and $S_{M_O}(M_O, t_{i+1})$ are each the enabling mappings of E_M , E_{M_I} , and E_{M_O} , respectively.

Let

$$\begin{aligned} S_{ou}(ou(t_i), Tu_h(t_i)) &= E_M, \\ S_{oq}(oq(t_i), Tq_h(t_i)) &= E_{M_I}, \\ S_{or}(or(t_{i+1}), Tr_h(t_{i+1})) &= E_{M_O} \end{aligned}$$

Then, according to Definition 6, there exist information objects

$$\begin{aligned} Iu(t_i) &= \langle ou(t_i), Tu_h(t_i), Sou, M, t_i, S_M \rangle, \\ Iq(t_i) &= \langle oq(t_i), Tq_h(t_i), Soq, M_I, t_i, S_{M_I} \rangle, \\ Ir(t_{i+1}) &= \langle or(t_{i+1}), Tr_h(t_{i+1}), Sor, M_O, t_{i+1}, S_{M_O} \rangle \end{aligned}$$

such that

$$\begin{aligned} &S_{or}(or(t_{i+1}), Tr_h(t_{i+1})) \\ &\subseteq Cn(S_{ou}(ou(t_i), Tu_h(t_i)) \cup S_{oq}(oq(t_i), Tq_h(t_i))) \end{aligned}$$

Thus, the necessity of the first part of the theorem is established.

On the other hand, for any $1 \leq i \leq n-1$, suppose there exist information objects $Iu(t_i) = \langle ou(t_i), Tu_h(t_i), Sou, M, t_i, S_M \rangle$, $Iq(t_i) = \langle oq(t_i), Tq_h(t_i), Soq, M_I, t_i, S_{M_I} \rangle$, and $Ir(t_{i+1}) = \langle or(t_{i+1}), Tr_h(t_{i+1}), Sor, M_O, t_{i+1}, S_{M_O} \rangle$, such that in the formal system \mathcal{L} ,

$$\begin{aligned} &S_{or}(or(t_{i+1}), Tr_h(t_{i+1})) \\ &\subseteq Cn(S_{ou}(ou(t_i), Tu_h(t_i)) \cup S_{oq}(oq(t_i), Tq_h(t_i))) \end{aligned}$$

Then, according to Lemma A.1, $E_M = S_{ou}(ou(t_i), Tu_h(t_i))$, $E_{M_I} = S_{oq}(oq(t_i), Tq_h(t_i))$, and $E_{M_O} = S_{or}(or(t_{i+1}), Tr_h(t_{i+1}))$ are interpretations of \mathcal{L} over the three finite domains $ou(t_i) \times Tu_h(t_i)$, $oq(t_i) \times Tq_h(t_i)$, and $r(t_{i+1}) \times Tr_h(t_{i+1})$, respectively, and $E_{M_O} \subseteq Cn(E_M \cup E_{M_I})$. At the same time, $S_M(M, t_i)$, $S_{M_I}(M_I, t_i)$, and $S_{M_O}(M_O, t_{i+1})$ are the enabling mappings of E_M , E_{M_I} , and E_{M_O} , respectively. By Definition 4, the output $S_{M_O}(M_O, t_{i+1})$

of model M under the input $S_{M_I}(M_I, t_i)$ is interpretable in the formal system \mathcal{L} . Therefore, the sufficiency of the first part of the theorem is established.

For all $i = 1, \dots, n - 1$, by combining Definition 4 with the first part of the theorem, the second part of the theorem follows directly. This completes the proof.

Definition 4 provides a rigorous mathematical definition of model interpretability. Furthermore, Theorem 1 demonstrates that, throughout the processes of model construction and application, as long as the ontological states of the model and its input and output information can be established within the same formal system, it is possible to reveal the causal relationships between model inputs and outputs within this system, thereby achieving model interpretability. It should also be noted that formal systems vary greatly across different academic disciplines, and the myriad entities in the world can be expressed through information in the forms of formulas, code, text, graphics, or even video. Moreover, the same state can be represented in different information modalities according to varying user requirements. Therefore, Definition 4 and Theorem 1 theoretically establish a foundation for the flexible use of multiple information modalities and for providing model interpretability tailored to user needs.

5.2 Theorem of Ethical Safety Assurance

To apply the MLT-MF framework, it is first necessary to identify the corresponding well-formed ethical constraint formulas Ec in accordance with fundamental ethical standards such as fairness and privacy protection, thereby establishing a formalized expression of ethical security.

Definition 5 (Ethical Safety) Let $S(X, T)$ be the interpretation of a set of well-formed formulas in a formal system \mathcal{L} over the domain $X \times T$. Let $Ec(\vec{v})$ denote an ethical constraint expressed as a well-formed formula in \mathcal{L} , where $\vec{v} = (v_1, \dots, v_n)$ are its free variables. For each substitutable $(x, t) \in X \times T$, define

$$Ec|_{(x,t)} = Ec(\vec{v} \mapsto \vec{\sigma}(x, t)) \quad (5.2)$$

where $\vec{\sigma} : X \times T \rightarrow D^n$ is a value vector function such that $\sigma_i(x, t) \in D$ is the concrete value assigned to v_i for $1 \leq i \leq n$.

If for all $\varphi \in Cn(S(X, T))$, and all $(x, t) \in X \times T$,

$$\varphi \rightarrow \sim Ec|_{(x,t)} \quad (5.3)$$

does not hold, then $S(X, T)$ is said to be ethically safe with respect to Ec . Furthermore, if a model M is capable of producing output I , and both the ontological and carrier states of I are ethically safe with respect to Ec , then M is said to be ethically safe with respect to Ec .

In the definition of ethical safety, we require not only that $S(X, T)$ contains no formulas that entail $\sim Ec|_{(x,t)}$, but also that its logical closure $Cn(S(X, T))$ contains no such formulas. This is because if $Cn(S(X, T))$ were to include formulas entailing $\sim Ec|_{(x,t)}$, then the conjunction of multiple formulas in $S(X, T)$ could still violate the ethical constraint Ec . This would indicate that $S(X, T)$ implicitly allows situations that contravene Ec , which must be strictly avoided in a rigorous sense. Moreover, it is generally not difficult for a model M to achieve ethical safety with respect to Ec in a simple manner; the key challenge

lies in ensuring the largest possible set of valid outputs while maintaining ethical safety. To this end, we propose:

Theorem 2 (Ethical Safety Assurance) Suppose model M is capable of processing Iq with Iu and outputting Ir . Let $S_{or}(or, Tr_h)$ denote the ontological state of Ir . For any ethical constraint Ec represented by a well-formed formula in \mathcal{L} , there exists a constructive algorithm for obtaining the largest output state subset $S_{or}^{Ec}(or, Tr_h) \subseteq S_{or}(or, Tr_h)$ that is ethically safe with respect to Ec . By introducing an ethical safeguard formula for Ec into Iu , it is thereby possible to ensure that model M attains the maximal output state that is ethically safe with respect to Ec .

Proof: Since model M is capable of processing Iq with Iu and outputting Ir , for the ontological states $S_{ou}(ou, Tu_h)$, $S_{oq}(oq, Tq_h)$ and $S_{or}(or, Tr_h)$ of Iu , Iq and Ir respectively, the MLT-MF framework provides:

$$\begin{aligned}
 \varphi_u := & ((\forall \Phi_u)(\forall \Phi_q)(IsSubsetOf^2(\Phi_u, S_{ou}(ou, Tu_h)) \\
 & \wedge IsSubsetOf^2(\Phi_q, S_{oq}(oq, Tq_h)) \\
 & \wedge Processable^2(\Phi_u, \Phi_q)) \\
 \rightarrow & (\exists \varphi_r(IsFormulaOf^2(\varphi_r, S_{or}(or, Tr_h)) \\
 & \wedge Eq^2(\varphi_r, f_{process}^2(\Phi_u, \Phi_q))))).
 \end{aligned} \tag{5.4}$$

Thus, the set

$$\begin{aligned}
 S_{or}(or, Tr_h) = \{ \varphi_r \mid & \varphi_r = Processable^2(\Phi_u, \Phi_q), \\
 & \Phi_u \in Sou(ou, Tu_h), \\
 & \Phi_q \in Soq(oq, Tq_h) \}
 \end{aligned} \tag{5.5}$$

represents the theoretical output states of model M .

Since $S_{or}(or, Tr_h)$ is a finite set, we construct a finite hypergraph

$$H_{or} = (S_{or}(or, Tr_h), \mathcal{E}) \tag{5.6}$$

where the vertex set is precisely $S_{or}(or, Tr_h)$, and the hyperedge set \mathcal{E} covers all well-formed formulas that directly or implicitly violate the ethical constraint Ec :

(1) For any $\varphi_r \in S_{or}(or, Tr_h)$ and $(x, t) \in or \times Tr_h$, if $\varphi_r \rightarrow \sim Ec|_{(x,t)}$, then add the hyperedge $\{\varphi_r\}$ to \mathcal{E} ;

(2) If there exists a minimal subset $W \subseteq S_{or}(or, Tr_h)$ such that the conjunction of all formulas in W entails $\sim Ec|_{(x,t)}$, then add the hyperedge W to \mathcal{E} .

Let G be an independent set in H_{or} , i.e., a subset of vertices containing no hyperedge $e \in \mathcal{E}$. If there exists $\varphi \in Cn(G)$ such that

$$\varphi \rightarrow \sim Ec|_{(x,t)} \tag{5.7}$$

then there must exist a finite subset $\{\varphi_{r_1}, \dots, \varphi_{r_k}\} \subseteq G$ such that $\varphi_{r_1} \wedge \dots \wedge \varphi_{r_k} = \varphi$, and hence $\varphi_{r_1} \wedge \dots \wedge \varphi_{r_k} \rightarrow \sim Ec|_{(x,t)}$. Let $W = \{\varphi_{r_1}, \dots, \varphi_{r_k}\}$, so the conjunction of W entails $\sim Ec|_{(x,t)}$.

According to the hyperedge construction rules, if $|W| = 1$, then W itself directly violates Ec , and there must be a hyperedge $\{\varphi r_1\}$. But since $\{\varphi r_1\} \in G$, this contradicts the assumption that G is an independent set. If $|W| \geq 2$, then by the compactness theorem, the logical entailment can be captured by a finite minimal subset, so there exists a minimal subset $W_{\min} \subseteq W$ whose conjunction entails $\sim Ec|_{(x,t)}$. Therefore, there exists a hyperedge $W_{\min} \subseteq W \subseteq G$ in H_{or} , again contradicting the independence of G . Thus, (4.7) cannot hold, and the independent set G is ethically safe with respect to Ec .

By the maximum independent set theorem for finite hypergraphs, H_{or} necessarily contains an independent set G_{\max} of maximal cardinality. Suppose there exists another ethically safe subset K with

$$|K| > |G_{\max}| \quad (5.8)$$

then K cannot contain any hyperedge $e \in \mathcal{E}$. Otherwise, if $|e| = 1$, then K directly violates Ec ; if $|e| \geq 2$, then the formulas in K violate Ec . Both cases contradict the ethical safety assumption for K . Therefore, K must also be an independent set in H_{or} , and (5.8) cannot hold. Hence, G_{\max} is the largest ethically safe subset of $S_{or}(or, Tr_h)$ with respect to Ec .

Let $S_{or}^{Ec}(or, Tr_h) = G_{\max}$ and $S_{or}^{\sim Ec}(or, Tr_h) = S_{or}(or, Tr_h) \setminus S_{or}^{Ec}(or, Tr_h)$. In addition, introduce a new constant in \mathcal{L} : NEc , representing a non- Ec ethical safety prompt, and a new predicate: $IsSafeback^1(NEc)$, indicating that M outputs the non- Ec ethical safety prompt NEc . We may safely assume that \mathcal{L} originally contains neither.

In this way, add to $Sou(ou, Tu_h)$ an ethical safeguard formula:

$$\begin{aligned} \varphi u = & (\forall \varphi r)(IsFormulaOf^2(\varphi r, S_{or}(or, Tr_h))) \rightarrow \exists \varphi s (IsFormulaOf^2(\varphi s, S_{os}(os, Ts_h)) \\ & \wedge (IsFormulaOf^2(\varphi r, S_{or}^{Ec}(or, Tr_h)) \rightarrow Eq^2(\varphi s, \varphi r)) \\ & \wedge (IsFormulaOf^2(\varphi r, S_{or}^{\sim Ec}(or, Tr_h)) \rightarrow Eq^2(\varphi s, IsSafeback^1(NEc)))) \end{aligned} \quad (5.9)$$

Since the newly added φu pertains to $S_{os}(os, Ts_h)$ and is entirely independent of the existing formulas in $Sou(ou, Tu_h)$, it does not affect the satisfaction of Postulate 5 by $Sou(ou, Tu_h)$. Moreover,

$$S_{os}(os, Ts_h) = S_{or}^{Ec}(or, Tr_h) \cup \{IsSafeback^1(NEc)\} \quad (5.10)$$

Because NEc and $IsSafeback^1(NEc)$ were not previously present in \mathcal{L} , and $S_{or}^{Ec}(or, Tr_h)$ and $\{IsSafeback^1(NEc)\}$ are logically independent and both logically consistent, $S_{os}(os, Ts_h)$ is also logically consistent and satisfies all other conditions of Postulate A.1. Therefore, it is the maximal output state that is ethically safe with respect to Ec .

By taking $S_{os}(os, Ts_h)$ as the ontological state and mapping it via recoverable information Is to the carrier state $S_M(M, Ts_m)$, $S_M(M, Ts_m)$ is necessarily also ethically safe with respect to Ec . This satisfies the condition in Definition 5 for model M to be ethically safe with respect to Ec . The theorem is thus proved.

Theorem 2 not only establishes that it is possible to construct an ethical safety assurance mechanism for models, but also provides a constructive algorithm—based on hypergraphs—

for obtaining the maximum ethically safe output. However, computing the maximum independent set in a hypergraph is generally an NP-hard problem. In practical applications, the algorithm can be simplified by leveraging two functions: one for ranking the conflict intensity among formulas in S_{or} (or, Tr_h), and another for ethical safety checking, thus yielding an approximately maximal safe output. This is a practical issue that warrants further investigation and will not be elaborated upon here. Meanwhile, the inheritance of ethical safety in the learning process can be achieved by incorporating dedicated ethical constraint regularization terms into the model algorithm. This involves more specific model structures and algorithmic design, which are beyond the scope of this paper.

In summary, based on the MLT-MF framework, Definition 10 and Theorem 5, for the first time, construct a formal theoretical framework for ethical safety. This approach, unlike those based on heuristic rules or statistical indicators, fills the gap in mathematical foundations and verifiability in traditional research, and provides concrete methodological guidance for the automated embedding and verification of ethical constraints.

5.3 Theorem on TVD Upper Bounds

Applying the MLT-MF framework allows us to estimate upper bounds on the generalization error measured by Total Variation Distance (TVD) between model distributions, facilitating the analysis and prediction of model generalization performance across a variety of tasks.

Theorem 3 (TVD Upper Bound for Conservative Prediction Strategies in Noise-Free Inputs and Uncovered Training Regions) Let the information describing the model M after learning and optimization be $I_u = \langle ou, Tu_h, S_{ou}, M, Tu_m, S_M \rangle$, and the input information be $I_q = \langle oq, Tq_h, S_{oq}, cq, Tq_m, S_{cq} \rangle$. Assume both S_{ou} and S_{oq} are distributed according to probability distributions over the same measurable space. Let $|S_{oq}|$ and $|S_{ou} \cap S_{oq}|$ denote the cardinalities of the finite sets S_{oq} and $S_{ou} \cap S_{oq}$, respectively. The probability distribution of the model is $p_M(x)$, where $p_M(x) > 0$ for $x \in S_{ou}$; the distribution over S_{oq} is $p_q(x)$, with $p_q(x) > 0$ for $x \in S_{oq}$. The total probability mass of $p_q(x)$ over $S_{ou} \cap S_{oq}$ is denoted P_{Mq} . When the model M is sufficiently trained on S_{ou} , and adopts a conservative uniform prediction for unknown states, the total variation distance between $p_M(x)$ and $p_q(x)$ satisfies:

$$TVD(p_q, p_M) = \begin{cases} \approx 0, & \text{if } S_{oq} \subset S_{ou} \\ \leq \sqrt{\frac{1}{2}((1 - P_{Mq}) \log((|S_{oq}| - |S_{ou} \cap S_{oq}|)/(1 - P_{Mq})) - H(p_q))}, & \text{if } S_{oq} \not\subset S_{ou} \cap S_{oq} \end{cases} \quad (5.11)$$

For the second case, it is assumed that $S_{oq} \setminus S_{ou} \neq \emptyset$, $1 - P_{Mq} > 0$, and $|S_{oq}| - |S_{ou} \cap S_{oq}| > 0$. Here, $H(p_q) = -\sum_{x \in S_{oq} \setminus S_{ou}} p_q(x) \log p_q(x)$ is the entropy of the data in the non-overlapping region.

Proof: Since M is sufficiently trained on S_{oq} within the overlapping region $S_{ou} \cap S_{oq}$, and adopts a conservative uniform distribution to predict unknown states, $p_M(x)$ closely approximates $p_q(x)$ in the overlapping region $S_{ou} \cap S_{oq}$, and follows a uniform distribution over the non-overlapping region $S_{oq} \setminus S_{ou}$. That is,

$$p_M(x) = \begin{cases} \approx p_q(x), & \text{if } x \in S_{ou} \cap S_{oq} \\ \frac{1-P_{Mq}}{|S_{oq}|-|S_{ou} \cap S_{oq}|}, & \text{if } x \in S_{oq} \setminus S_{ou} \end{cases} \quad (5.12)$$

Using KL-divergence to measure the difference between the true distribution and the hypothesized model distribution, we have (Kullback and Leibler, 1951):

$$\begin{aligned} D_{KL}(p_q(x) \parallel p_M(x)) &= \sum_{x \in S_{oq}} p_q(x) \log \frac{p_q(x)}{p_M(x)} \\ &= \sum_{x \in S_{ou} \cap S_{oq}} p_q(x) \log \frac{p_q(x)}{p_M(x)} + \sum_{x \in S_{oq} \setminus S_{ou}} p_q(x) \log \frac{p_q(x)}{p_M(x)} \end{aligned} \quad (5.13)$$

According to (5.12), in the overlapping region,

$$\begin{aligned} \sum_{x \in S_{ou} \cap S_{oq}} p_q(x) \log \frac{p_q(x)}{p_M(x)} &\approx \sum_{x \in S_{ou} \cap S_{oq}} p_q(x) \log \frac{p_q(x)}{p_q(x)} \\ &= 0 \end{aligned} \quad (5.14)$$

This establishes the first case in (5.11).

In the non-overlapping region, the true distribution $p_q(x)$ can be arbitrary. Similarly, by (5.12), we have

$$\begin{aligned} \sum_{x \in S_{oq} \setminus S_{ou}} p_q(x) \log \frac{p_q(x)}{p_M(x)} &= \sum_{x \in S_{oq} \setminus S_{ou}} p_q(x) \log p_q(x) - \sum_{x \in S_{oq} \setminus S_{ou}} p_q(x) \log p_M(x) \\ &= -H(p_q) - \sum_{x \in S_{oq} \setminus S_{ou}} p_q(x) \log \frac{(1-P_{Mq})}{|S_{oq}|-|S_{ou} \cap S_{oq}|} \\ &= -H(p_q) - \log \frac{(1-P_{Mq})}{|S_{oq}|-|S_{ou} \cap S_{oq}|} \sum_{x \in S_{oq} \setminus S_{ou}} p_q(x) \\ &= (1-P_{Mq}) \log \frac{|S_{oq}|-|S_{ou} \cap S_{oq}|}{1-P_{Mq}} - H(p_q) \end{aligned} \quad (5.15)$$

Since both $p_M(x)$ and $p_q(x)$ are probability distributions defined on the same measurable space, we can use KL-divergence to estimate an upper bound on their total variation distance. By Pinsker's inequality (Pinsker, 1964), we have: ...

$$\begin{aligned} TVD(p_q, p_M) &\leq \sqrt{\frac{1}{2} D_{KL}(p_q(x) \parallel p_M(x))} \\ &= \sqrt{\frac{1}{2} \left(\sum_{x \in S_{ou} \cap S_{oq}} p_q(x) \log \frac{p_q(x)}{p_M(x)} + \sum_{x \in S_{oq} \setminus S_{ou}} p_q(x) \log \frac{p_q(x)}{p_M(x)} \right)} \\ &\approx \sqrt{\frac{1}{2} \left((1-P_{Mq}) \log \frac{|S_{oq}|-|S_{ou} \cap S_{oq}|}{1-P_{Mq}} - H(p_q) \right)} \end{aligned} \quad (5.16)$$

This establishes the second case in (5.11).

Since we have already assumed that the carrier states $S_M(M, Tu_m)$ and $S_{cq}(cq, Tq_m)$ of $Iu = \langle ou, Tu_h, Sou, M, Tu_m, S_M \rangle$ and $Iq = \langle oq, Tq_h, Soq, cq, Tq_m, S_{cq} \rangle$ are both represent the physical realizations of S_{ou} and S_{oq} in model M and its interface, respectively. It follows that equation (5.11) characterizes the upper bound of the model's TVD. This completes the proof.

Distinct from traditional generalization theories such as VC dimension and Rademacher complexity, Theorem 3, based on the MLT-MF framework, utilizes P_{Mq} and $|S_{oq}| - |S_{ou} \cap S_{oq}|$ —which reflect the overlap between test data and the model's original information—as well as the entropy $H(p_q)$ of test data in the non-overlapping region, as evaluation metrics to provide an explicit quantitative estimation of the TVD. Since TVD reflects the degree of distributional alignment of the model, independent of specific models and tasks, it is generally applicable for analyzing training performance. Moreover, for classification tasks with 0-1 loss, the upper bound of the generalization error is equivalent to the TVD (Devroye et al., 2013), while for regression tasks, the upper bound of the generalization error is given by the product of the TVD and the Lipschitz loss (Devroye et al., 2013). Therefore, TVD serves as an indicator for estimating a model's generalization error. In this way, Theorem 3 offers a novel perspective and practical guidance for model design and training data acquisition.

In general, input information is inevitably affected by noise, and arbitrary predictive strategies can be adopted in regions not covered by training data. According to Definition 3 on structural decomposition of noisy information, we can thus obtain more general results regarding the model's TVD.

Theorem 4 (TVD Upper Bound for Arbitrary Prediction Strategies with Noisy Inputs and Uncovered Training Regions) Let the base space X be a finite set. The training information domain of the model M is $S_{ou} \subseteq X$. The true problem domain is $S_{oq} \subseteq X$, and the true distribution p_q satisfies $\sum_{x \in S_{oq}} p_q(x) = 1$. The noisy information ontological state $\widetilde{S}_{oq} = S_{oq} \setminus S_{oq}^- \cup S_{oq}^+$, as defined in Definition 3, replaces S_{oq} as the actual input to the model M . The noise loss probability mass is $P_l = \sum_{x \in S_{oq}^-} p_q(x) \in [0, 1]$, and the noise addition probability mass is $P_a = \sum_{x \in S_{oq}^+} p^+(x) \in [0, 1]$, where p^+ is a non-negative kernel on the noise addition region, satisfying $1 - P_l + P_a > 0$. The distribution of the noisy input \widetilde{S}_{oq} is given by $\widetilde{p}_q(x) = (p_q(x) \bullet 1\{x \notin S_{oq}^-\} + p^+(x) \bullet 1\{x \in S_{oq}^+\}) / (1 - P_l + P_a)$. Let $V = \widetilde{S}_{oq} \setminus S_{ou}$ denote the region not covered by training information, with uncovered probability mass $P_{uncov} = \sum_{x \in V} \widetilde{p}_q(x) \in [0, 1]$. The conditional distribution on V is $r(x) = \widetilde{p}_q(x) / P_{uncov}$ (and when $P_{uncov} = 0$, all terms involving V below are taken as 0). The predictive strategy p_0 on the uncovered region V is an arbitrary distribution, satisfying $\sum_{x \in V} p_0(x) = 1, p_0(x) \geq 0$. The model distribution p_M is determined by training on the covered region $U = \widetilde{S}_{oq} \cap S_{ou}$, and on V , $p_M(x) = P_{uncov} p_0(x)$. Assume that the model's fitting error on the covered region is $E_{fit} = D_{KL}(\widetilde{p}_q|_U \parallel p_M|_U)$, where $\widetilde{p}_q|_U$ and $p_M|_U$ denote the distributions restricted to U and normalized (under the ideal conditions assumed in Theorem 3, E_{fit} tends to zero).

Thus, the upper bound of the TVD for model M with respect to noisy input information is given by $TVD(\widetilde{p}_q, p_M) \leq \sqrt{\frac{[E_{fit} + P_{uncov} D_{KL}(r \parallel p_0)]}{2}}$ (5.17)

The upper bound of the TVD for model M with respect to the true information is

$$TVD(p_q, p_M) \leq \begin{cases} P_l + \sqrt{\frac{[E_{fit} + P_{uncov} D_{KL}(r \| p_0)]}{2}}, & \text{if } P_l \geq P_a, \\ \frac{P_a}{1 - P_l + P_a} + \sqrt{\frac{[E_{fit} + P_{uncov} D_{KL}(r \| p_0)]}{2}}, & \text{if } P_l < P_a. \end{cases} \quad (5.18)$$

Proof: Based on the conditions provided in the theorem, we have:

$$\begin{aligned} D_{KL}(\tilde{p}_q \| p_M) &= \sum_{x \in \widetilde{S_{oq}^-}} \tilde{p}_q(x) \log \frac{\tilde{p}_q(x)}{p_M(x)} \\ &= \sum_{x \in U} \tilde{p}_q(x) \log \frac{\tilde{p}_q(x)}{p_M(x)} + \sum_{x \in V} \tilde{p}_q(x) \log \frac{\tilde{p}_q(x)}{p_M(x)} \\ &= D_{KL}(\tilde{p}_q|U \| p_M|U) + \sum_{x \in V} P_{uncov} r(x) \log \frac{P_{uncov} r(x)}{P_{uncov} p_0(x)} \\ &= E_{fit} + P_{uncov} D_{KL}(r \| p_0) \end{aligned} \quad (5.17)$$

Here, E_{fit} reflects the degree of fit of M on the region covered by the training information, and its probabilistic upper bound can be characterized by measures such as VC dimension, Rademacher complexity, or training stability. Moreover, by applying Pinsker's inequality, the first conclusion of the theorem can be obtained:

$$TVD(\tilde{p}_q, p_M) \leq \sqrt{\frac{D_{KL}(\tilde{p}_q \| p_M)}{2}} = \sqrt{\frac{[E_{fit} + P_{uncov} D_{KL}(r \| p_0)]}{2}} \quad (5.18)$$

Since the distribution of the noisy input $\widetilde{S_{oq}}$ is

$$\tilde{p}_q(x) = \frac{p_q(x) \bullet 1\{x \notin S_{oq}^-\} + p^+(x) \bullet 1\{x \in S_{oq}^+\}}{1 - P_l + P_a} \quad (5.19)$$

It follows that

$$\begin{aligned} TVD(p_q, \tilde{p}_q) &= (\sum_{x \in X} |p_q(x) - \tilde{p}_q(x)|) / 2 \\ &= (\sum_{x \in S_{oq}^-} |p_q(x) - \tilde{p}_q(x)| + \sum_{x \in S_{oq}^+} |p_q(x) - \tilde{p}_q(x)| + \sum_{x \in X \setminus (S_{oq}^- \cup S_{oq}^+)} |p_q(x) - \tilde{p}_q(x)|) / 2 \\ &= (\sum_{x \in S_{oq}^-} |p_q(x)| + \sum_{x \in S_{oq}^+} |p^+(x)| / (1 - P_l + P_a) + \sum_{x \in X \setminus (S_{oq}^- \cup S_{oq}^+)} |p_q(x) - p_q(x)| / (1 - P_l + P_a)) / 2 \\ &= (P_l + \frac{P_a}{1 - P_l + P_a} + \frac{|P_l - P_a| \sum_{x \in X \setminus (S_{oq}^- \cup S_{oq}^+)} p_q(x)}{1 - P_l + P_a}) / 2 = (P_l + \frac{P_a}{1 - P_l + P_a} + \frac{|P_l - P_a|(1 - P_l)}{1 - P_l + P_a}) / 2 \\ &= \begin{cases} P_l, & \text{if } P_l \geq P_a, \\ \frac{P_a}{1 - P_l + P_a}, & \text{if } P_l < P_a. \end{cases} \quad (5.22) \end{aligned}$$

By applying the triangle inequality, we have

$$\begin{aligned} TVD(p_q, p_M) &\leq TVD(p_q, \tilde{p}_q) + TVD(\tilde{p}_q, p_M) \\ &\leq \begin{cases} P_l + \sqrt{\frac{[E_{fit} + P_{uncov} D_{KL}(r \| p_0)]}{2}}, & \text{if } P_l \geq P_a, \\ \frac{P_a}{1 - P_l + P_a} + \sqrt{\frac{[E_{fit} + P_{uncov} D_{KL}(r \| p_0)]}{2}}, & \text{if } P_l < P_a. \end{cases} \quad (5.23) \end{aligned}$$

Thus, the second conclusion of the theorem is established, completing the proof.

Theorem 4 unifies the noise structure, coverage geometry, and uncovered-region strategies within a computable TVD upper bound framework. Specifically, the TVD upper bounds for model M with respect to both noisy actual inputs and true inputs are expressed in terms of the noise loss mass P_l , addition mass P_a , fitting error over the covered region E_{fit} , uncovered mass P_{uncov} , and the KL divergence $D_{KL}(r \| p_0)$ between the conditional distribution on the uncovered region and the prediction strategy. This formulation reveals several important insights: the loss and addition masses determine the deviation between the true target

and the noisy target; the fit over the covered region, the coverage structure, and the divergence between the conditional distribution and prediction strategy on the uncovered region jointly determine the model's deviation from the noisy target. Consequently, the effects of noise deletion/addition on target deviation can be directly assessed. This upper bound provides actionable guidance for the joint optimization of training coverage and prediction strategies, and can undoubtedly be applied more broadly to the analysis and optimization of model performance.

6 Experimental Results

Using the feedforward neural network model listed in Appendix C, we conducted regression experiments on two bivariate root functions: $y_1 = \sqrt{4x_1^2 + 3x_2^2}$ and $y_2 = \sqrt{2x_1^2 + x_2^2}$. Both the training and test datasets were specific. We evaluated the models' prediction errors under various conditions, assessed the impact and computational cost of ethical and safety mechanisms, and explored the challenge of providing multiple types of explanations for the same output. These experiments serve to illustrate and validate the definitions and theorems presented in Section 5.

6.1 Experiments on the TVD upper bound under noiseless input and conservative prediction strategy

To evaluate the TVD upper bound estimation of Theorem 3 under noiseless input and conservative prediction strategy, as well as its relationship to model performance, we construct the following experimental setup. On the (x_1, x_2) plane, we select a square region centered at $(1.0, 1.0)$ with side length 1, and uniformly sample 10,000 points as the training dataset. For the test dataset, we uniformly sample 10,000 points within a circular region centered at $(1.5, 1.0)$ with radius 0.5. The model learning rate is set to $\eta = 0.01$. By uniformly sampling 10,000 points within the test region and computing the corresponding discrete points in the (y_1, y_2) plane using the target function, we approximate the distribution $p_q(x)$ of the test dataset and its entropy function. Fig. 3 illustrates the experimental conditions and outcomes:

- (a) The overlap rate between the test and training datasets is approximately 50%.
- (b) For 10 randomly selected samples from the overlapping region, as the number of training steps increases from 10 to 4000 (i.e., as the model becomes more sufficiently trained), the root mean square error (RMSE) of the model's predictions steadily approaches zero. This result aligns with the first case of Theorem 3, equation (5.11).
- (c) For all test samples from the non-overlapping region, a conservative uniform prediction strategy was used. For almost all samples (except a few outliers), their RMSE is less than $TVD \approx \sqrt{((1 - 0.4951) \ln((10000 - 4951)/(1 - 0.4951)) - 2.9741)/2} \approx 0.9155$. This indicates that even in regression tasks, although TVD is not strictly equivalent to generalization error, it can still effectively capture the distributional characteristics of generalization error.
- (d) For 10 randomly selected test samples from the non-overlapping region, when using the model's prediction method, the RMSE also decreases with more training steps, reflecting a certain degree of model generalization outside the training data region. However, the rate of error reduction is significantly lower than in the overlapping region, and for some samples,

the RMSE remains higher than that of the conservative uniform prediction. In fact, when training is insufficient, the overall RMSE of the model’s predictions can even exceed the TVD. Meanwhile, the RMSE of conservative predictions for these samples is much lower than the TVD, reflecting the conclusion of the second case in Theorem 3, equation (5.11).

In summary, this regression experiment using a simple feedforward neural network model demonstrates and validates the accuracy of the model TVD upper bound estimation based on the MLT-MF framework, and its potential for estimating generalization error. Since the theoretical proof of Theorem 3 is independent of specific models and tasks, it promises to be extensible to more complex scenarios.

6.2 Experimental Evaluation of the TVD Upper Bound under Noisy Input and Arbitrary Prediction Strategy

To evaluate Theorem 4’s estimation of the TVD upper bound under conditions of noisy input and the adoption of arbitrary prediction strategies in regions not covered by the training data, as well as its relationship to model performance, we utilize the same model instance, training dataset, and test dataset as in the previous experiment. We introduce noise into the input by locally adding or deleting noise information in the test dataset according to Definition 3, so that the model input contains noise. Meanwhile, in the regions not covered by the training data, we apply an arbitrary prediction strategy based on the joint distribution $p_0(x)$ formed by two independent normal distributions, $N \sim (0.6306, 0.4585^2)$ and $N \sim (0.4031, 0.3666^2)$, to process and predict the input data. Fig. 3: (a) The training dataset S_{ou} (selected within the blue square) and the test dataset S_{oq} (selected within the red circle) are the same as those used in the experiment described in Section 6.1. The upper arc-shaped segment of S_{oq} is shifted upward, and the vacated region, denoted as S_{oq}^- , is excluded from the test input. The shifted portion, S_{oq}^+ , does not overlap with the original test dataset but partially overlaps with S_{ou} ; it is added as new noisy test data. This structure satisfies the definition of noisy input, $\tilde{S}_{oq} = S_{oq} \setminus S_{oq}^- \cup S_{oq}^+$.

(b) For the noisy test dataset comprising 11,034 samples, we compute the probability distribution for each test sample using the same method as in Section 6.1. The loss mass is $P_l = 0.0744$, the addition mass is $P_a = 0.0517$, the uncovered mass is $P_{uncov} = 0.5091$, and the KL divergence is $D_{KL}(r \parallel p_0) = 45.58$. This yields a TVD upper bound between the noisy input distribution and the model distribution of 3.312. By randomly selecting 100 groups of samples from the test dataset and inputting them into the model after 20 training steps, we find that the root mean square error (RMSE) of all outputs (marked by blue dots) is less than the TVD upper bound indicated by the red line. This validates the conclusion of Theorem 4, Equation (5.17).

(c) In the above example, $P_l = 0.0744 > 0.0517 = \gamma$. Under the same conditions, we randomly select 100 samples from the noiseless test dataset, convert them into corresponding noisy data as input to the model, and find that the RMSE of all outputs remains below the TVD upper bound of 3.4555. This validates the case where $P_l \geq P_a$ as given in Theorem 4, Equation (5.18).

(d) To examine the case where $P_l < P_a$ in Theorem 4, Equation (5.18), we construct a new noisy test dataset comprising 10,000 samples. In this case, $P_l = 0.0744$, $P_a = 0.1551$, $P_{uncov} = 0.5530$, and $D_{KL}(r \parallel p_0) = 40.88$, resulting in a TVD upper bound of 3.4325.

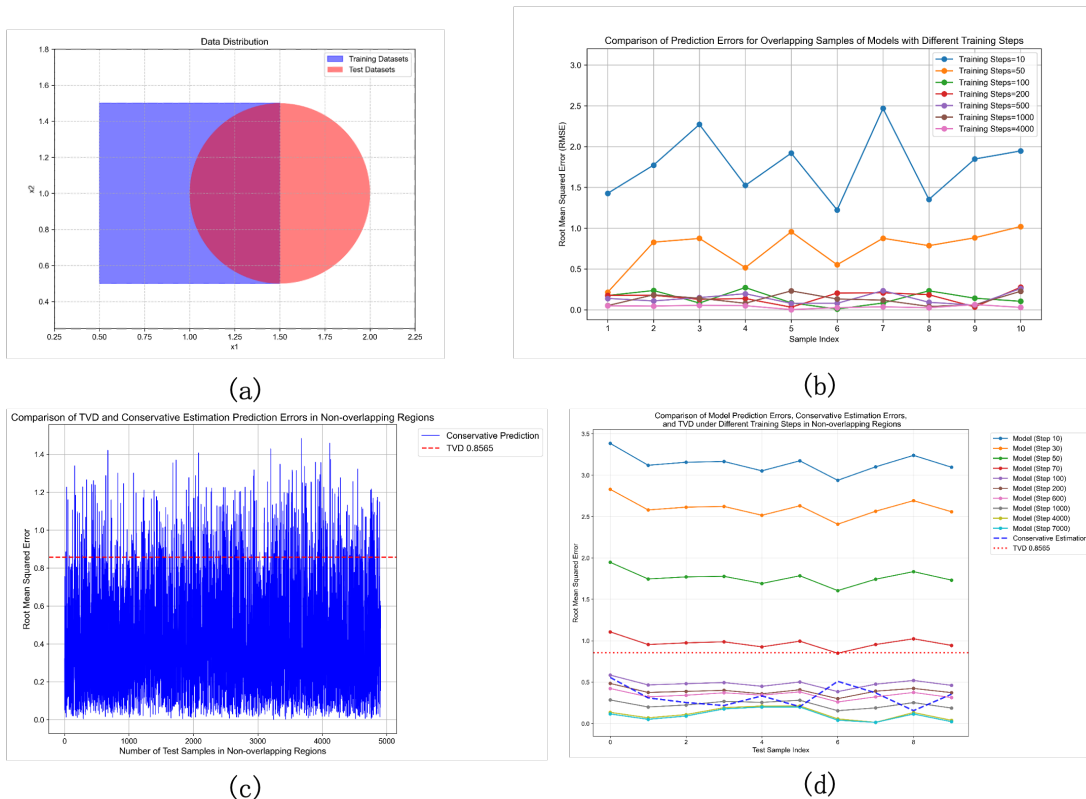


Figure 3: **Experimental Evaluation and Results of the TVD Upper Bound under Noiseless Input and Conservative Prediction Strategy.** (a) The blue rectangular region represents the training dataset comprising 10,000 samples, while the red circular region represents the test dataset, also with 10,000 samples. Among these, 4,951 samples overlap with the training set. (b) For each of the training steps (10, 50, 100, 200, 500, 1000, 4000), the variation in root mean square error (RMSE) is shown for 10 randomly selected test samples from the training dataset. (c) In the non-overlapping region between the test and training datasets, the RMSEs for all 5,049 test samples are compared between the conservative uniform prediction strategy and the TVD upper bound. (d) For 10 randomly selected test samples from the non-overlapping region, the changes in RMSE are shown for training steps (10, 30, 300, 600, 1000, 4000, 7000), along with comparisons to both the TVD upper bound and the RMSE from the conservative uniform prediction.

Again, by randomly selecting 100 samples from the noiseless test dataset and converting them into noisy inputs for the model, the RMSE of all outputs remains below the TVD upper bound indicated by the red line, thereby confirming the corresponding conclusion provided by Theorem 4.

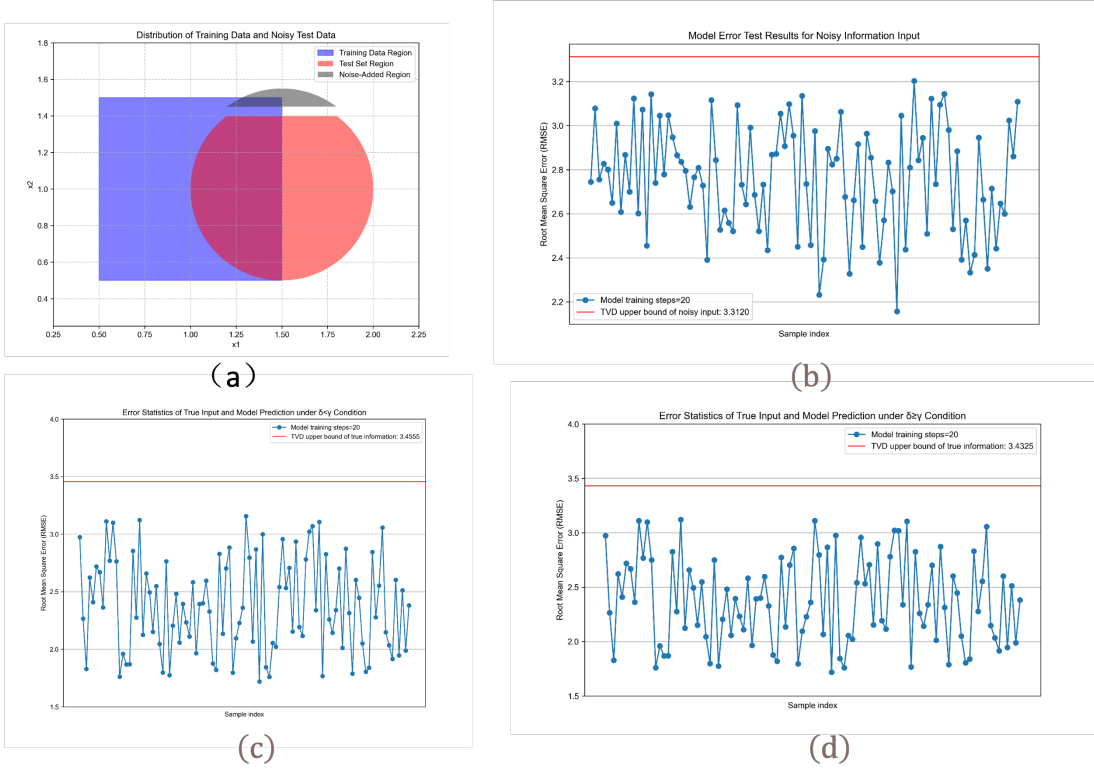


Figure 4: Experimental Evaluation and Results of the TVD Upper Bound under Noisy Input and Arbitrary Prediction Strategy. **(a)** The upper arc-shaped region of the test dataset is shifted upward, and the resulting vacant region is excluded from the test input. The shifted segment, which does not overlap with the original test dataset, is incorporated as noise into the new test dataset. **(b)** One hundred groups of samples are randomly selected from the noisy test dataset and processed by the model. The RMSE of the predictions are represented by 100 points along the blue line, while the red line indicates the TVD upper bound between the noisy input distribution and the model distribution. **(c)** In the case of $P_l \geq P_a$, 100 samples are randomly selected from the noiseless test dataset, transformed into the corresponding noisy data, and processed by the model. The RMSE of each prediction is represented by 100 points along the blue line, with the red line denoting the TVD upper bound between the noiseless input distribution and the model distribution. **(d)** In the case of $P_l < P_a$, 100 samples are randomly selected from the noiseless test dataset, transformed into the corresponding noisy data, and processed by the model. The RMSE of each prediction is represented by 100 points along the blue line, with the red line indicating the TVD upper bound between the noiseless input distribution and the model distribution.

Through these experiments, we have comprehensively validated Theorem 4 regarding the TVD upper bound under noisy input and arbitrary prediction strategies. Furthermore,

as illustrated in Fig. 4, there remains a noticeable gap between the RMSE of the model outputs and the TVD upper bound across various scenarios, indicating that the upper bound provided by Theorem 4 is still somewhat conservative. Further research may yield tighter error estimates under typical conditions.

6.3 Ethical Safety Assurance Experiment

Given the nature of the bivariate root function regression task, the model’s predicted outputs should never be negative. This requirement is analogous to Definition 5, which ensures that model outputs do not violate the ethical constraints Ec . Therefore, using the same training dataset as in the previous prediction error experiments, we set the learning rate to $\eta = 0.001$ and trained the model for 165 steps. For testing, we generated a dataset of 10,000 samples with (x_1, x_2) drawn uniformly from within a circle of radius 0.5 centered at $(-1, -1)$. The criterion for judging ethical safety violations was whether the model’s predicted output was negative. This setup was used to test the feasibility of Theorem 2 and to evaluate the additional computational overhead introduced by ethical safety checking.

For each trial, 5,000 test samples were randomly selected using the trial number as a random seed. Two types of tests were conducted in parallel: “Without Ethical Safety Check” and “With Ethical Safety Check.” In the “Without Ethical Safety Check” condition, model predictions were output directly and the total computation time was recorded. In the “With Ethical Safety Check” condition, each prediction was first checked for sign; if any prediction was negative, an ethical error message was output, otherwise, the model’s prediction was output. The total computation time was also recorded in this scenario. In total, 10 trials were conducted, and the results are shown in Table 1.

Table 1: Summary Table of Ethical Safety Experiment Results

Trial Number	Time w/o Check (s)	Time w/ Check (s)	Time Ratio	Safe Samples	Warning Samples	Safe Rate	Warning Rate
1	0.367	0.391	1.063	4517	483	100%	100%
2	0.365	0.378	1.036	4521	479	100%	100%
3	0.352	0.362	1.030	4548	452	100%	100%
4	0.330	0.378	1.146	4516	484	100%	100%
5	0.371	0.383	1.032	4523	477	100%	100%
6	0.327	0.380	1.160	4546	454	100%	100%
7	0.358	0.402	1.123	4545	455	100%	100%
8	0.360	0.410	1.140	4538	462	100%	100%
9	0.361	0.365	1.010	4519	481	100%	100%
10	0.355	0.424	1.192	4533	467	100%	100%

In Table 1, the “Computation Time Ratio” is calculated as the computation time with ethical safety checking divided by the computation time without it. For the simple feedforward neural network model used in these experiments, the additional computational overhead for performing ethical safety checks before model output ranged from 1.0% to 19.2%. As model size increases, this overhead is expected to decrease in proportion; however, as

the number of ethical safety constraints grows, the overhead will increase accordingly. This is a key consideration for implementing ethical safety in models. In these 10 trials, more than 19% of samples resulted in unethical predictions. In every trial, both the ‘‘Correct Prediction Rate for Safe Outputs’’ and the ‘‘Correct Prompt Rate for Unethical Outputs’’ were 100%, demonstrating that by incorporating safety checks and informative outputs, we can always guarantee the ethical safety of model predictions while maximizing the number of safe outputs.

In summary, this ethical safety experiment, grounded in Definition 5 and the formal MLT-MF-based framework for ethical safety, illustrates and validates Theorem 2 regarding the feasibility of integrating ethical safety checking mechanisms and achieving the maximal number of safe outputs.

6.4 Interpretability Experiment

For our bivariate root regression task, the output should never be negative. However, in the ethical safety assurance experiment, after 165 training steps, the model produced negative predictions for more than 19% of randomly selected 5,000-sample test batches, repeated over 10 trials. According to Theorem 1, this phenomenon can be explained from multiple perspectives, each based on different information.

6.4.1 MATHEMATICAL OPERATION-BASED EXPLANATION

After 165 training steps, the neural network model M has the following weight matrices and bias vectors from the input layer to the hidden layer:

$$W_1 \approx \begin{bmatrix} -0.065 & -0.429 \\ 0.681 & -0.157 \\ -0.498 & -0.586 \end{bmatrix}, \quad b_1 \approx \begin{bmatrix} 0.129 \\ -0.551 \\ 0.350 \end{bmatrix} \quad (6.1)$$

The weights and biases from the hidden layer to the output layer are:

$$W_2 \approx \begin{bmatrix} 0.145 & 0.519 & -0.423 \\ 0.022 & 0.048 & 0.043 \end{bmatrix}, \quad b_2 \approx \begin{bmatrix} 0.613 \\ 0.199 \end{bmatrix} \quad (6.2)$$

Therefore, for the test sample $X = [-1.3535, -1.3535]^T$, the model predicts:

$$Y = \begin{bmatrix} y_1 \\ y_2 \end{bmatrix} = \text{Identity}(W_2 \text{ReLU}(W_1 X + b_1) + b_2) \approx \begin{bmatrix} -0.040 \\ 0.277 \end{bmatrix} \quad (6.3)$$

Here, $y_1 = -0.040 < 0$, which mathematically explains why model M outputs a negative value for input X .

These formulas provide the designer’s mathematical representation of the model’s computational process. They are equivalent to the formal forward propagation rules (C.21) and (C.22) in Appendix C. According to the OIT perspective, these equations describe the ontological state of the model, its outputs, and the information they convey. The model, along with its input and output mechanisms, serves as the carrier of this information and realizes the computational process. Therefore, using these formulas to explain why the model produces negative outputs satisfies the requirements of Definition 4 regarding model

interpretability and meets the needs of researchers who seek to understand model behavior from a mathematical standpoint.

6.4.2 VISUALIZATION-BASED EXPLANATION OF THE COMPUTATIONAL PROCESS

Depicting the model’s computational process visually can make explanations of model behavior much more intuitive. To this end, for model M after 165 training steps, we illustrate its complete structure—covering the inputs, internal neural network calculations and data flow, and outputs—in Fig. 5.

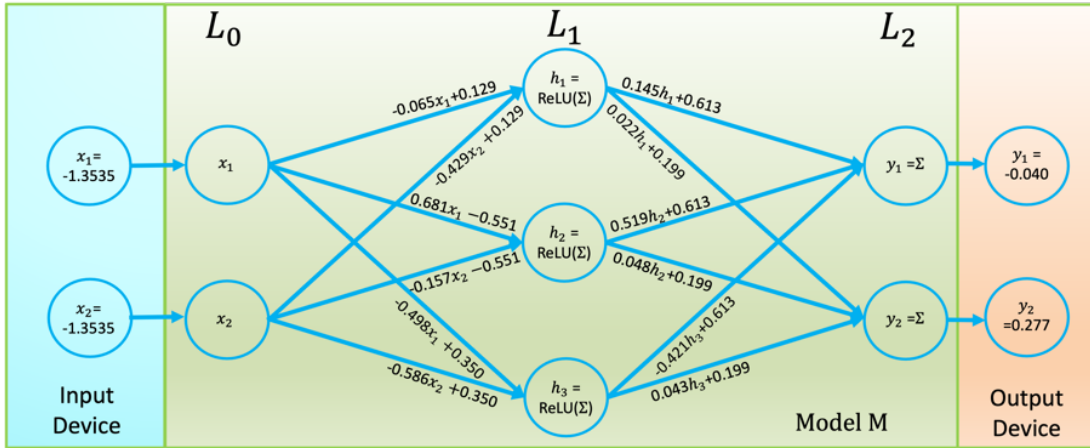


Figure 5: Schematic diagram of the computational process for model M after 165 training steps, showing its handling of the input sample $X = [-1.3535, -1.3535]^T$ and output $Y \approx [-0.040, 0.277]^T$.

Compared with equations (6.1)–(6.3), Fig. 5 not only comprehensively reflects the input, weight matrices, bias vectors, neuron activation functions, and the specific data and formulas for outputs, but also highlights the interactions between the input/output devices and the model. The figure offers a more direct view of the internal data processing pipeline, making it easier to examine and verify each step of the computation. Thus, the visualization provides a more accessible and concrete explanation of how model M processes inputs and generates results.

6.4.3 PARTITION-BASED EXPLANATION

It is evident that equations (6.1)–(6.3) and Fig. 5 explain only the result of model M processing the specific sample $X = [-1.3535, -1.3535]^T$. They do not account for the phenomenon observed in the ethical safety assurance experiment, where each random selection of 5,000 samples from the test dataset yields over 19% negative predictions. To explain this, a broader statistical analysis across more data samples is needed.

Fig. 6(a) provides a visual depiction of the decision boundary after 165 training steps, showing where model M predicts negative outputs. Notably, there is a boundary line approximately passing through points $(-2.0, -0.4)$ and $(-0.4, -2.0)$. For samples on the upper

right side of this diagonal, model M consistently predicts non-negative values; for those on the lower left, the model consistently outputs negative values. The red region in the figure, representing the test dataset, falls precisely on the lower left side of this boundary line, which explains why a random selection of 5,000 samples from the test set will always include a substantial portion that triggers negative predictions. This visual and statistical partitioning thus provides an intuitive explanation for the observed frequency of negative outputs in the ethical safety experiment.

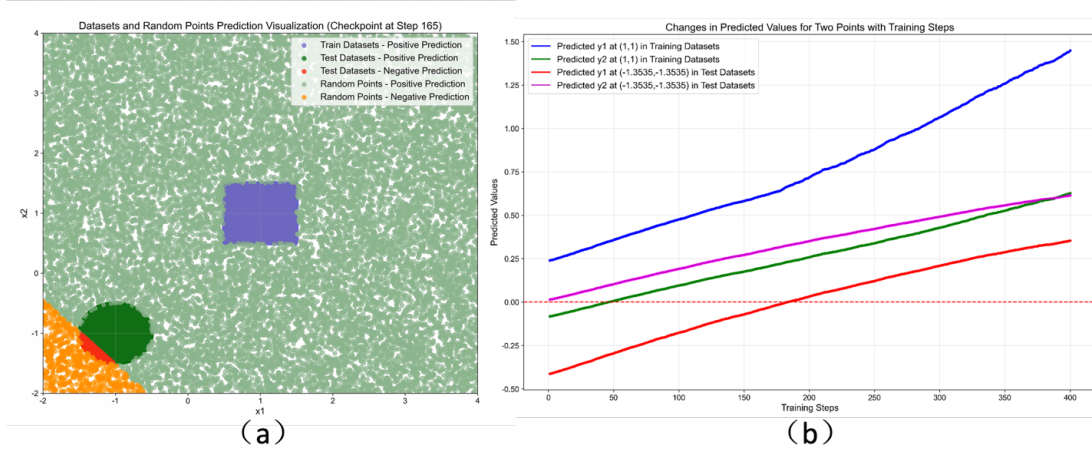


Figure 6: Illustration of Prediction Polarity and Impact of Training Steps. **(a)** Polarity distribution of predicted data around the training set region after model M has been trained for 165 steps. The blue square marks the area where the training dataset is located, centered at (1, 1) with a side length of 1. Green dots indicate samples with all-positive predictions; dark green dots indicate samples with all-positive predictions that also belong to the test set; red dots indicate samples with at least one negative prediction that belong to the test set; orange dots indicate samples with at least one negative prediction that do not belong to the test set. **(b)** Cumulative effect of up to 400 training steps on the prediction polarity at two points: (1, 1) and (-1.3535, -1.3535). The blue and green lines represent the predicted y_1 and y_2 values for the sample (1, 1) from the training set; the red and pink lines represent the predicted y_1 and y_2 values for the sample (-1.3535, -1.3535) from the test set.

Fig. 6(a) presents an overall view of numerous inputs processed and predicted by model M. This visualization also represents an ontological state of M as it handles a wide range of input information—the real processing and prediction procedure of M is a direct result of this ontological mapping. Thus, according to Definition 4, Figure 5(a) constitutes a valid explanation for the distribution of prediction polarities by M.

6.4.4 EXPLANATION BASED ON CUMULATIVE TRAINING EFFECTS

The previous three explanations all focus on the behavior of M after 165 training steps. However, model training is a continuous process of cumulative improvement. Examining only the model's instantaneous performance at a particular training step cannot fully explain the causes of abnormal outputs. To address this, we further trained M for 400 iterations on the training dataset. Fig. 6(b) shows the predictions for both $(1, 1)$ and $(-1.3535, -1.3535)$ after each training step.

It is clear that even for $(1, 1)$ — a central sample from the training set—the predicted y_2 by M remains negative during roughly the first 50 training steps. Only after more than 50 steps does the prediction move away from negative values. For the test sample $(-1.3535, -1.3535)$, it takes more than about 180 training steps before the prediction begins to consistently avoid negative values. This cumulative effect is entirely due to the optimization of M 's parameters as training progresses.

In fact, by applying the forward propagation rules (C.21) and (C.22) from the appendix—substituting the model parameters obtained after each training step—one can, through a recursive process, provide a rigorous and step-by-step explanation for M 's predictions on specific input samples after any given amount of training.

7 Discussion and Conclusion

This work, grounded in the Objective Information Theory (OIT), develops the MLT-MF framework, employing a formal logical system to integrate the complete causal chain of model construction, training, input processing, output, and online learning. Under a unified semantics, we propose formal definitions of model interpretability and ethical safety, derive two classes of explicit TVD upper bound theorems, and validate the framework through experiments with feedforward neural network models. The core contributions are as follows:

(1) Enabled Mapping for Information Transmission: We characterize the mathematical mapping and the dual physical-causal nature of information transfer from ontological states to carrier states through the concept of “enabled mapping.” This is further extended to chain transmission, mapping each engineering stage of model development to a segment of the information chain, such that model behavior, training, and inference are reduced to logically verifiable compositions of mappings.

(2) Unified Representation of Interpretability and Safety: By adopting higher-order formal logic as a unified representation of “state,” we propose necessary and sufficient conditions for interpretability—linking input, output, and model within the same formal system via logical closure—and construct maximal safe outputs for ethical safety based on hypergraph maximum independent sets.

(3) Integration of Statistical Error, Noise Structure, and Coverage Geometry: We integrate statistical learning error characterization with information noise structure and training coverage geometry, providing a closed-form TVD upper bound, and operationally decomposing it in terms of coverage fitting error, uncovered mass, KL divergence, and noise deletion/addition terms.

Therefore, this study addresses two longstanding gaps in machine learning theory: the lack of unified semantics and causal chain constraints across different stages, and the absence of verifiable mathematical definitions and constructive guarantees for ethical safety

and interpretability. By unifying the “existence–transmission–realization” of information within formal logical explanations, we rigorously establish that model interpretability corresponds to information existence, thereby providing a logical-theoretical foundation for translating ethical safety from normative requirements into decidable and constructible guarantees. Using TVD as a fundamental measure of distributional alignment, and establishing correspondences with practical engineering concerns such as training coverage gaps, uncovered-region prediction strategies, and noise deletion/addition, this work bridges the gap between abstract generalization theory and data coverage/system implementation, thus connecting statistical learning, mathematical logic, information science, and systems engineering.

All conclusions and methods presented are amenable to engineering implementation:

- **Interpretability** can be realized at multiple levels through unified formal systems, including mathematical formulas, dataflow diagrams, and parameter representations, which is especially important for high-risk industries.
- **Ethical safety** is implemented via conflict detection and maximal independent set approximation of output propositions, enabling a deployable process for maximal safe outputs.
- **TVD bounds** can be integrated into data auditing and training monitoring KPIs: noise loss mass δ and addition mass γ can be obtained from data collection/cleaning audits; uncovered mass P_{uncov} can be estimated by OOD detection; coverage fitting error E_{fit} can be approximated by validation sets; and KL divergence $D_{KL}(r \parallel p_0)$ can be estimated via density ratios or energy models. These provide quantitative guidance for training data coverage planning, uncovered-region prediction strategy design, and data denoising, enabling a closed-loop for the joint optimization of “data–strategy–model.”

Of course, this work has limitations: the current formal system is most transparent for finite discrete sets, and further refinement is needed for continuous, time-varying, multimodal, and multi-agent scenarios, particularly regarding measurability and dynamic consistency. The maximal independent set for ethical safety is generally NP-hard, requiring the development of complexity-controlled approximation algorithms and alignment with business ethics standards. TVD upper bounds rely on conservative inequalities such as Pinsker’s; in typical scenarios, error estimates may be tightened using related theoretical advances. Physical causality in enabled mappings calls for interdisciplinary integration with various branches of physics, leveraging parameters such as energy consumption, latency, and uncertainty to advance from qualitative causality to quantitative verification. Future work may include large-scale empirical studies to verify the observability of TVD upper bounds and the benefits of strategy optimization, as well as further development of cross-modal and multi-agent information chain composition and conflict resolution methods, thereby enhancing the universality and practical value of MLT-MF in complex systems.

Acknowledgments and Disclosure of Funding

Junxuan He from Beijing University of Posts and Telecommunications implemented all the experiments described in the paper according to the author’s ideas, producing complete model code and training/test datasets, providing indispensable and strong support for illustrating and validating the theorems related to MLT-MF. The author offers special thanks for his hard work, keen understanding, and efficient implementation. During the writing and revision of this paper, I received many insightful comments from Associate Professor Wang Rui of the School of Computer Science at Shanghai Jiao Tong University. I also gained much inspiration and assistance from regular academic discussions with doctoral students Siyuan Qiu, Chun Li, Hu Xu, and Zeyan Li. I hereby express my sincere gratitude to them.

Data and Code availability

All datasets and codes used in this work are available at <https://github.com/xuhu6736/MLT-MF>.

References

- Josh Achiam, Steven Adler, Sandhini Agarwal, Lama Ahmad, Ilge Akkaya, Florencia Leoni Aleman, Diogo Almeida, Janko Altenschmidt, Sam Anderson, Costin Anitescu, et al. Gpt-4 technical report. *arXiv preprint arXiv:2303.08774*, 2023. doi: 10.48550/arXiv.2303.08774.
- Pierre Alquier. User-friendly introduction to pac-bayes bounds. *Foundations and Trends® in Machine Learning*, 17(2):174–303, 2024.
- Christopher Burr and David Leslie. Ethical assurance: a practical approach to the responsible design, development, and deployment of data-driven technologies. *AI and Ethics*, 3(1):73–98, 2023.
- Aakanksha Chowdhery, Sharan Narang, Jacob Devlin, Maarten Bosma, Gaurav Mishra, Adam Roberts, Paul Barham, Hyung Won Chung, Charles Sutton, Sebastian Gehrmann, et al. Palm: Scaling language modeling with pathways. *Journal of Machine Learning Research*, 24(240):1–113, 2023.
- Luc Devroye, László Györfi, and Gábor Lugosi. *A probabilistic theory of pattern recognition*, volume 31. Springer Science & Business Media, 2013.
- Editorial Committee of Dictionary of Mathematics. *Dictionary of Mathematics, Volume V*. China Science and Technology Press, August 2002.
- Artur d’Avila Garcez and Luis C Lamb. Neurosymbolic ai: The 3rd wave. *Artificial Intelligence Review*, 56(11):12387–12406, 2023.
- Claire Glanois, Paul Weng, Matthieu Zimmer, Dong Li, Tianpei Yang, Jianye Hao, and Wulong Liu. A survey on interpretable reinforcement learning. *Machine Learning*, 113(8):5847–5890, 2024.

- Suriya Gunasekar, Yi Zhang, Jyoti Aneja, Caio César Teodoro Mendes, Allie Del Giorno, Sivakanth Gopi, Mojan Javaheripi, Piero Kauffmann, Gustavo de Rosa, Olli Saarikivi, et al. Textbooks are all you need. *arXiv preprint arXiv:2306.11644*, 2023. doi: 10.48550/arXiv.2306.11644.
- Alan G Hamilton. *Logic for mathematicians*. Cambridge University Press, 1988.
- Richard Hawkins, Colin Paterson, Chiara Picardi, Yan Jia, Radu Calinescu, and Ibrahim Habli. Guidance on the assurance of machine learning in autonomous systems (amlas). *arXiv preprint arXiv:2102.01564*, 2021.
- Solomon Kullback and Richard A Leibler. On information and sufficiency. *The Annals of Mathematical Statistics*, 22(1):79–86, 1951.
- Zachary C Lipton. The mythos of model interpretability: In machine learning, the concept of interpretability is both important and slippery. *Queue*, 16(3):31–57, 2018.
- Giuseppe Marra, Francesco Giannini, Michelangelo Diligenti, and Marco Gori. From statistical relational to neurosymbolic artificial intelligence: A survey. *Artificial Intelligence*, 328:104062, 2024. ISSN 0004-3702. doi: 10.1016/j.artint.2023.104062.
- Tim Miller. Explanation in artificial intelligence: Insights from the social sciences. *Artificial intelligence*, 267:1–38, 2019.
- Aadarsh Pant, Rashina Hoda, Chakkrit Tantithamthavorn, and Burak Turhan. Ethics in ai through the practitioner’s view: a grounded theory literature review. *Empirical Software Engineering*, 29:67, 2024. doi: 10.1007/s10664-024-10465-5.
- Mark Semenovitch Pinsker. *Information and information stability of random variables and processes*. Holden-Day, 1964.
- Cynthia Rudin. Stop explaining black box machine learning models for high stakes decisions and use interpretable models instead. *Nature machine intelligence*, 1(5):206–215, 2019.
- Stuart Russell, Daniel Dewey, and Max Tegmark. Research priorities for robust and beneficial artificial intelligence. *AI magazine*, 36(4):105–114, 2015.
- Bernhard Schölkopf, Francesco Locatello, Stefan Bauer, Nan Rosemary Ke, Nal Kalchbrenner, Anirudh Goyal, and Yoshua Bengio. Toward causal representation learning. *Proceedings of the IEEE*, 109(5):612–634, 2021.
- Claude E Shannon. The mathematical theory of communication. *Bell System Technical Journal*, 27(3):379–423, 1948.
- Ravid Shwartz-Ziv and Naftali Tishby. Opening the black box of deep neural networks via information. *arXiv preprint arXiv:1703.00810*, 2017.
- Mitul Harishbhai Tilala, Krupa Patel, Foram Patel, Ravi Doshi, and Rajesh M Rawal. Ethical considerations in the use of artificial intelligence and machine learning in health care: a comprehensive review. *Cureus*, 16(6), 2024.

- Hugo Touvron, Louis Martin, Kevin Stone, Peter Albert, Amjad Almahairi, Yasmine Babaei, Nikolay Bashlykov, Soumya Batra, Prajjwal Bhargava, Shruti Bhosale, et al. Llama 2: Open foundation and fine-tuned chat models. *arXiv preprint arXiv:2307.09288*, 2023. doi: 10.48550/arXiv.2307.09288.
- Vladimir N Vapnik. An overview of statistical learning theory. *IEEE Transactions on Neural Networks*, 10(5):988–999, 1999. doi: 10.1109/72.788640.
- Jianfeng Xu. Research and application of general information measures based on a unified model. *IEEE Transactions on Computers*, 2024. doi: 10.1109/TC.2024.3349650.
- Jianfeng Xu, Zhongzhi Zhang, Aolin Xu, and Cangqing Wang. Objective information theory: A sextuple model and 9 kinds of metrics. In *2014 Science and information conference*, pages 793–802. IEEE, 2014. doi: 10.1109/SAI.2014.6918277.
- Jianfeng Xu, Chuanren Liu, Zhongzhi Zhang, and Cangqing Wang. General information metrics for improving ai model training efficiency. *Artificial Intelligence Review*, 58:289, 2025. doi: 10.1007/s10462-025-11281-z.
- Xiangxiang Xu, Shao-Lun Huang, Lizhong Zhang, and Qiuling Yan. An information theoretic interpretation to deep neural networks. *Entropy*, 24(1):135, 2022.
- Yechao Zhang, Shengshan Hu, Yu Leo, Junyu Hou, Xiaogeng Liu, Zhan Qin, Ming Li, and Hai Wang. Why does little robustness help? a further step towards understanding adversarial transferability. In *2024 IEEE Symposium on Security and Privacy (SP)*, pages 3365–3384. IEEE, 2024.

Appendix A. Appendix A. Formal Representation of States

The postulates of information emphasize that the state of the ontology enables a mapping to the state of the carrier. Therefore, establishing a formal representation of both ontological and carrier states is particularly important.

Definition A.1 (Higher-Order Formal Logical System): Suppose a formal system \mathcal{L} is described using the following symbol set:

- Variables x_1, x_2, \dots ;
- Individual constants a_1, a_2, \dots ;
- Functions $f_1^1, f_2^1, \dots, f_1^2, f_2^2, \dots, f_1^3, f_2^3, \dots$;
- Parentheses $(,)$;
- Predicates $A_1^1, A_2^1, \dots, A_1^2, A_2^2, \dots, A_1^3, A_2^3, \dots$;
- Logical connectives “not” \sim , “implication” \rightarrow ;
- Quantifier “for all” \forall .

A term in \mathcal{L} is defined as follows:

- (1) Variables and individual constants are terms;
- (2) If f_i^n ($n > 0, i > 0$) is a function in \mathcal{L} , and t_1, \dots, t_n are terms in \mathcal{L} that do not contain f_i^n itself, then $f_i^n(t_1, \dots, t_n)$ is also a term in \mathcal{L} ;
- (3) If A_i^n ($n > 0, i > 0$) is a predicate in \mathcal{L} , and t_1, \dots, t_n are terms in \mathcal{L} that do not contain A_i^n itself, then $A_i^n(t_1, \dots, t_n)$ is also a term in \mathcal{L} ;
- (4) The set of all terms in \mathcal{L} is generated by (1), (2), and (3).

Based on this, we can define atomic formulas in \mathcal{L} :

If A_i^n ($n > 0, i > 0$) is a predicate in \mathcal{L} and t_1, \dots, t_n are terms in \mathcal{L} not containing A_i^n itself, then $A_i^n(t_1, \dots, t_n)$ is an atomic formula in \mathcal{L} .

We then define well-formed formulas (WFFs) in \mathcal{L} :

- (5) Every atomic formula in \mathcal{L} is a WFF;
- (6) If \mathcal{A} and \mathcal{B} are WFFs in \mathcal{L} , then $\sim \mathcal{A}$, $\mathcal{A} \rightarrow \mathcal{B}$, $(\forall x_i)\mathcal{A}$, $(\forall f_i^n)\mathcal{A}$, and $(\forall A_i^n)\mathcal{A}$ are all WFFs in \mathcal{L} , where x_i, f_i^n, A_i^n are variables, functions, and predicates in \mathcal{L} , respectively, and no predicate or function symbol is applied, either directly or indirectly, to itself;
- (7) The set of all WFFs in \mathcal{L} is generated by (5) and (6).

The higher-order formal logical system \mathcal{L} defined here, based on the flexibility of predicate logic, can describe various relationships and constraints among states. Its recursive structure and higher-order quantification support the nested definition of complex data and behaviors, and it explicitly prohibits any predicate or function symbol from applying to itself—directly or indirectly—to avoid self-referential paradoxes.

For simplicity, \mathcal{L} does not define connectives such as “and” \wedge , “or” \vee , “if and only if” \leftrightarrow , or the quantifier “exists” \exists , and other commonly used logical symbols. However, mathematical logic theory demonstrates that these symbols are entirely equivalent to appropriate combinations of existing symbols and can make many formulas more concise (Hamilton, 1988). Therefore, they are introduced as defined symbols in subsequent discussions.

Definition A.2 (Interpretation of a Formal System) An interpretation E of a formal system \mathcal{L} over a domain D_E assigns specific values to constants, elements of the domain D_E to variables, and turns function and predicate symbols into functions and predicates over that domain D_E , thereby yielding a set of WFFs each with a truth value.

Definition A.2 assigns concrete values and meaning to a set of formulas in a formal system \mathcal{L} through interpretation, thereby providing a fundamental approach for formally describing the definitional, attributive, structural, relational, and evolutionary state properties of objects in both the subjective and objective worlds.

Postulate A.1 (Expression of Object States) The state set of an object collection over a specified time set is constituted by its attributes—such as properties, structures, values, and relations—as well as the evolution rules and logical combinations among these attributes, and satisfies the following conditions:

- (1) **Domain invariance:** definitions of the object set and time set remain unchanged.
- (2) **Numerical determinacy:** concrete numerical values determine values of certain properties and forms.
- (3) **Attribute expressibility:** properties, forms, values, relations are expressible via functions and predicates in a formal system satisfying Definition 2.
- (4) **Rule expressibility:** evolution rules among attributes are expressible in such a formal system using time variables and implication, and contain no implicit self-reference.
- (5) **Logical coherence:** no logical contradictions exist among attributes and rules, nor among any logical conjunctions thereof.

Lemma A.1 (Formal Expression of States) If the state set $S(X, T)$ of objects X over times T satisfies Postulate A.1, then it can be represented as an interpretation of a formal system \mathcal{L} over the domain $X \times T$, and it is logically coherent.

Proof: Since the state set $S(X, T)$ of the object set X over the time set T satisfies Postulate A.1, we construct the corresponding formal system \mathcal{L} as follows:

By (1), the definitions of the elements in X and T remain unchanged, ensuring determinacy. The variables in the formal system \mathcal{L} are defined to correspond to each element of $X \times T$, thus making $X \times T$ the domain of discourse for \mathcal{L} . Consequently, $S(X, T)$ has a well-defined domain.

By (2), the constants in \mathcal{L} are defined to represent all possible values in $S(X, T)$.

By (3), the functions and predicates in \mathcal{L} represent the properties, forms, values, and relations of X over T as captured in $S(X, T)$.

By (4), consider two ternary predicates A_1^3 and A_2^3 . Let $A_1^3(x_1, t_1, f_1^2(x_1, t_1))$ and $A_2^3(x_2, t_2, f_2^2(x_2, t_2))$ be two properties of $S(X, T)$ corresponding to objects $x_1, x_2 \in X$, times $t_1, t_2 \in T (t_1 < t_2)$, and binary functions $f_1(x_1, t_1), f_2(x_1, t_1)$. Suppose all $A_1^3(x_1, t_1, f_1^2(x_1, t_1))$ satisfy the rule of evolving from t_1 to t_2 into some $A_2^3(x_2, t_2, f_2^2(x_2, t_2))$. The formula $(\forall A_1^3 \forall f_1^2 \forall x_1 A_1^3(x_1, t_1, f_1^2(x_1, t_1)) \rightarrow \exists A_2^3 \exists f_2^2 \exists x_2 A_2^3(x_2, t_2, f_2^2(x_2, t_2)))$ is also a well-formed formula in \mathcal{L} , with respect to the interpretation of x_1, x_2, t_1, t_2 , and is able to express the corresponding rules in $S(X, T)$. For other rules in $S(X, T)$, the related elements in the domain $X \times T$ can similarly be interpreted and expressed via corresponding WFFs in \mathcal{L} , with no implicit logical self-reference.

Therefore, $S(X, T)$ constitutes an interpretation E of \mathcal{L} over the domain $X \times T$. By (5), both itself and its logical closure are logically consistent. The lemma is thus proved.

Lemma A.1 stipulates that the variables in \mathcal{L} are elements of $X \times T$; thus, in formulas, object and time elements appear in pairs (x, t) . In practice, some attributes may be time-invariant; then simplified expressions may be used to describe such attributes without time.

Appendix B. Appendix B. Finite Automaton States

Using the formal expression of states, we can study in depth the special and important object of finite automata (Xu, 2024).

Lemma B.1 (State Representation of Finite Automata) For any finite automaton M , one can describe its input, output, and state-transition behavior over a related time set T by the state set $S(M, T)$.

Proof: Let $M = \langle Q, R, U, \delta, \lambda \rangle$ be a finite automaton, and $T = \{t_i | i = 1, \dots, n\}$ the (strictly increasing) time points at which M performs input, output, or state-transition actions. By finite-automaton theory (Editorial Committee of Dictionary of Mathematics, 2002), $Q = \{q_{t_i} | i = 1, \dots, n-1\}$, $R = \{r_{t_i} | i = 2, \dots, n\}$, and $U = \{u_{t_i} | i = 1, \dots, n\}$ are nonempty finite sets of input symbols, output symbols, and states, respectively;

$\delta: U \times Q$ to U , is the next-state function;

$\lambda: U \times Q$ to R , is the output function.

For each state $u_{t_i} \in U$, define the state predicate $State^3$ by

$$\varphi_U(t_i) = State^3(M, t_i, u_{t_i}) \quad (B.1)$$

to assert that at time t_i , M is in state u_{t_i} , $i = 1, \dots, n$.

For each input $q_{t_i} \in Q$, define the input predicate $Input^3$ by

$$\varphi_I(t_i) = Input^3(M, t_i, q_{t_i}) \quad (B.2)$$

to assert that at time t_i , M receives input q_{t_i} , $i = 1, \dots, n-1$.

For each output $r_{t_i} \in R$, define the output predicate $Output^3$ by

$$\varphi_O(t_i) = Output^3(M, t_i, r_{t_i}) \quad (B.3)$$

to assert that at time t_i , M produces output r_{t_i} , $i = 2, \dots, n$.

The transition function δ is captured by the well-formed formula

$$\varphi_\delta(t_i) = \varphi_U(t_i) \wedge \varphi_I(t_i) \rightarrow \exists \delta(u_{t_i}, q_{t_i}) \wedge Eq^2(u_{t_{i+1}}, \delta(u_{t_i}, q_{t_i})) \wedge \varphi_U(t_{i+1}) \quad (B.4)$$

where the binary predicate $Eq^2(x, y)$ asserts $x = y$, $i = 1, \dots, n-1$.

Similarly, the output function λ is given by

$$\varphi_\lambda(t_i) = \varphi_U(t_i) \wedge \varphi_I(t_i) \rightarrow \exists \lambda(u_{t_i}, q_{t_i}) \wedge Eq^2(r_{t_{i+1}}, \lambda(u_{t_i}, q_{t_i})) \wedge IsElementof^2(r_{t_{i+1}}, R) \wedge \varphi_O(t_{i+1}) \quad (B.5)$$

where $IsElementof^2(x, X)$ asserts x is an element of X , $i = 1, \dots, n-1$.

Thus the state set

$$S(M, T) = \{\varphi_U(t_i), \varphi_I(t_j), \varphi_O(t_k), \varphi_\delta(t_j), \varphi_\lambda(t_j), \\ i = 1, \dots, n, j = 1, \dots, n-1, k = 2, \dots, n\} \quad (B.6)$$

describes M 's inputs, outputs, and state-transitions over T . Here $Cn(X)$ denotes the logical closure of the set of well-formed formulas X . This completes the proof.

It follows that every finite automaton can be formalized by the state set given in Theorem 2, which moreover exhibits automatic transition behavior. Hence we introduce:

Definition B.2 (Finite Automaton State) If a state set $S(X, T)$ expresses a finite automaton, then $S(X, T)$ is called a finite automaton state.

All practical information systems, including computing systems, are finite automata in the mathematical sense. Therefore, the concept of finite automaton state is of great significance in the study of machine learning.

Appendix C. Appendix C. Model Instance Validation of MLT-MF

To facilitate validation and illustration of the practical significance of MLT-MF and related theorems, we select a very simple model and use MLT-MF to establish formal representations with WFFs for each stage from initial information to training information, learning optimization, and processing/output.

C.1 A Simple Feedforward Neural Network Model

We choose a feedforward neural network M with an input layer containing two inputs, a hidden layer containing three neurons, and an output layer containing two outputs (Fig. C.1). Its simplicity helps explain the essence of MLT-MF in a clear and straightforward manner.

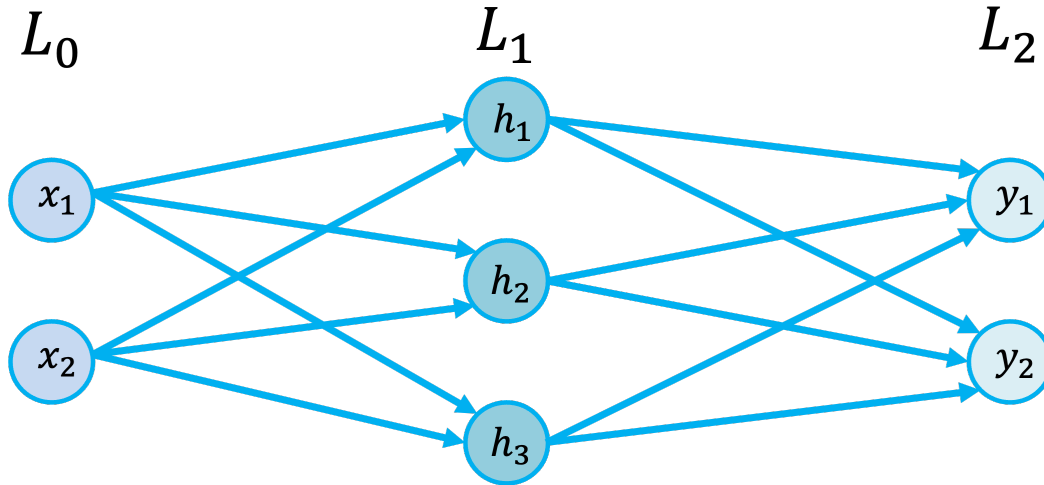


Figure 7: Fig. C.1 Schematic diagram of feedforward neural network model M

The hidden layer uses the ReLU activation function:

$$ReLU(x) = \max(0, x) \tag{C.1}$$

The output layer uses the identity activation:

$$Identity(x) = x \tag{C.2}$$

Initial weight matrices and bias vectors are defined between layers:

$$W_1 = \begin{bmatrix} w_{11}^1 & w_{12}^1 \\ w_{21}^1 & w_{22}^1 \\ w_{31}^1 & w_{32}^1 \end{bmatrix}, \quad b_1 = \begin{bmatrix} b_1^1 \\ b_2^1 \\ b_3^1 \end{bmatrix} \quad (\text{C.3})$$

$$W_2 = \begin{bmatrix} w_{11}^2 & w_{12}^2 & w_{13}^2 \\ w_{21}^2 & w_{22}^2 & w_{23}^2 \end{bmatrix}, \quad b_2 = \begin{bmatrix} b_1^2 \\ b_2^2 \end{bmatrix} \quad (\text{C.4})$$

Training or input data, output data, and training labels or target outputs are specified, with mean squared error (MSE) as the loss:

$$X = \begin{bmatrix} x_1 \\ x_2 \end{bmatrix}, \quad Y = \begin{bmatrix} y_1 \\ y_2 \end{bmatrix}, \quad Y_t = \begin{bmatrix} y_{t1} \\ y_{t2} \end{bmatrix} \quad \text{and} \quad Y_t = \text{Target}(X) \quad (\text{C.5})$$

$$L = \text{MSE}(Y, Y_t) = \frac{1}{2} \|Y - Y_t\|^2 = \frac{1}{2} ((y_1 - y_{t1})^2 + (y_2 - y_{t2})^2) \quad (\text{C.6})$$

The gradients of the loss function L with respect to the weight matrices and bias vectors are the primary basis for model M 's optimization during training. The four calculation formulas are as follows:

$$\nabla_{W_2} L = (Y - Y_t)(\text{ReLU}(W_1 X + b_1))^T \quad (\text{C.7})$$

$$\nabla_{b_2} L = (Y - Y_t) \quad (\text{C.8})$$

$$\nabla_{W_1} L = (W_2^T (Y - Y_t) \odot \text{ReLU}'(W_1 X + b_1)) X^T \quad (\text{C.9})$$

$$\nabla_{b_1} L = W_2^T (Y - Y_t) \odot \text{ReLU}'(W_1 X + b_1) \quad (\text{C.10})$$

In equations (C.9) and (C.10), the operator \odot denotes element-wise multiplication, and ReLU' represents the derivative of the ReLU function. Since ReLU is not differentiable at zero, we additionally define $\text{ReLU}'(0) = 0$. Thus, the update formulas for optimizing the weight matrices and bias vectors during M 's training are:

$$W_1^{\text{new}} = W_1 - \eta \nabla_{W_1} L, \quad b_1^{\text{new}} = b_1 - \eta \nabla_{b_1} L \quad (\text{C.11})$$

$$W_2^{\text{new}} = W_2 - \eta \nabla_{W_2} L, \quad b_2^{\text{new}} = b_2 - \eta \nabla_{b_2} L \quad (\text{C.12})$$

where η is the learning rate of M .

C.2 Symbol Definitions

MLT-MF uses a formal system to express the operational logic of each phase throughout the model's full lifecycle. Defining the symbols is a prerequisite for formal modeling. To this end, Tables C.1–C.4 provide definitions for the constants, variables, functions, and predicates used in the formal representation of model M .

C.3 Formal Representations of Information at Each Stage of Model M

Following MLT-MF, we build formal expressions for the following five stages:

(1) Initial information of M

Table 2: Definition of Constants

Symbol	Type	Definition
\mathbb{R}^2	Space	2-dimensional real space
\mathbb{R}^3	Space	3-dimensional real space

Table 3: Definition of Variables - Part I: Logical Formulas and Basic Variables

Symbol	Type	Definition
i, j, k	natural number	index or count
φo_i	WFFs	well-formed formulas in initial model ontological state
ψo_i	WFFs	well-formed formulas in initial model carrier state
φt_i	WFFs	well-formed formulas in training ontological state
ψt_i	WFFs	well-formed formulas in training carrier state
φu_i	WFFs	well-formed formulas in optimized model ontological state
ψu_i	WFFs	well-formed formulas in optimized model carrier state
φq_i	WFFs	well-formed formulas in input ontological state
ψq_i	WFFs	well-formed formulas in input carrier state
φr_i	WFFs	well-formed formulas in output ontological state
ψr_i	WFFs	well-formed formulas in output carrier state
φv_i	WFFs	well-formed formulas in re-optimized model ontological state
ψv_i	WFFs	well-formed formulas in re-optimized model carrier state
$layers$	natural number	number of layers in the model
v	real number	numerical values for weights and biases

According to the principles of OIT and based on MLT-MF, the model M is endowed with its initial information from the very beginning:

$$I_o = \langle oo, To_h, S_{oo}, M, To_m, S_M \rangle \quad (C.13)$$

Here, the ontology oo represents the designer's conceptual blueprint; To_h is the time at which the model is designed; and the ontological state $S_{oo}(oo, To_h)$ is a set of well-formed formulas that describe the initial operational logic of model M:

Table 4: Definition of Variables - Part II: Neural Network Parameters

Symbol	Type	Definition
$W_k^{(o)}$	matrix	weight matrix from k-th to (k+1)-th layer (initial)
$w_{ij}^{(o)k}$	real number	weight from j-th to i-th neuron (initial)
$b_k^{(o)}$	vector	bias vector of k-th layer (initial)
$b_i^{(o)k}$	real number	bias of i-th neuron in k-th layer (initial)
$W_k^{(u)}$	matrix	weight matrix from k-th to (k+1)-th layer (optimized)
$w_{ij}^{(u)k}$	real number	weight from j-th to i-th neuron (optimized)
$b_k^{(u)}$	vector	bias vector of k-th layer (optimized)
$b_i^{(u)k}$	real number	bias of i-th neuron in k-th layer (optimized)
$W_k^{(v)}$	matrix	weight matrix from k-th to (k+1)-th layer (re-optimized)
$w_{ij}^{(v)k}$	real number	weight from j-th to i-th neuron (re-optimized)
$b_k^{(v)}$	vector	bias vector of k-th layer (re-optimized)
$b_i^{(v)k}$	real number	bias of i-th neuron in k-th layer (re-optimized)
$W_k^{(w)}$	matrix	weight matrix from k-th to (k+1)-th layer (further re-optimized)
$w_{ij}^{(w)k}$	real number	weight from j-th to i-th neuron (further re-optimized)
$b_k^{(w)}$	vector	bias vector of k-th layer (further re-optimized)
$b_i^{(w)k}$	real number	bias of i-th neuron in k-th layer (further re-optimized)

$$S_{oo}(oo, To_h) = \{\varphi_{01}, \varphi_{02}, \varphi_{03}, \varphi_{04}, \varphi_{05}, \varphi_{06}, \varphi_{07}, \varphi_{08}, \varphi_{09}, \varphi_{10}, \varphi_{11}\} \quad (C.14)$$

The specific content of each formula is as follows:

- Network Structure Definition

$$\varphi_{01} = NetworkStructure^2(layers, 3) \wedge LayerSize^2(1, 2) \wedge LayerSize^2(2, 3) \wedge LayerSize^2(3, 2) \quad (C.15)$$

Table 5: Definition of Variables - Part III: Vectors and Optimization Parameters

Symbol	Type	Definition
X	vector	input vector
H	vector	hidden layer vector
Y	vector	output vector
Y_t	vector	output reference vector
x_i	real number	i-th element of input vector
h_i	real number	i-th element of hidden layer vector
y_i	real number	i-th element of output vector
y_{ti}	real number	i-th element of output reference vector
t	time	time point of state occurrence
δ	time	time step
L	real number	loss function value
$\nabla_{W_1}L$	real number	gradient of loss function w.r.t. W_1
$\nabla_{b_1}L$	real number	gradient of loss function w.r.t. b_1
$\nabla_{W_2}L$	real number	gradient of loss function w.r.t. W_2
$\nabla_{b_2}L$	real number	gradient of loss function w.r.t. b_2
η	positive real	learning rate

Table 6: Definition of Functions

Symbol	Number of Elements	Definition
$ReLU(x)$	1	rectified linear unit (ReLU) activation function
$Identity(x)$	1	identity function
\max	multivariate	maximum function
$MSE(Y, Y_t)$	2	mean squared error between vector Y and Y_t
$ReLU'(x)$	1	derivative of $ReLU(x)$
$Target(X)$	1	objective function for input vector X

- Weight Initialization

$$\varphi_{02} = \forall i \forall j (BelongsTo^2(i, \{1, 2, 3\}) \wedge BelongsTo^2(j, \{1, 2\}) \rightarrow \exists v (Eq^2(w_{ij}^{(o)1}, v))) \quad (C.16)$$

$$\varphi_{03} = \forall i \forall j (BelongsTo^2(i, \{1, 2\}) \wedge BelongsTo^2(j, \{1, 2, 3\}) \rightarrow \exists v (Eq^2(w_{ij}^{(o)2}, v))) \quad (C.17)$$

- Bias Initialization

Table 7: Definition of Predicates

Symbol	Definition
$NetworkStructure^2(layers, k)$	model structure has k layers
$LayerSize^2(k, j)$	the k-th layer has j neurons
$Eq^2(x, y)$	x equals y
$InputAt^2(X, t)$	input X at time t
$HiddenAt^2(H, t)$	hidden layer value is H at time t
$OutputAt^2(Y, t)$	output Y at time t
$InputAt^3(X, Y_t, t)$	input vector X and label vector Y_t at time t
$Differentiable^2(f, v)$	function f is differentiable with respect to v
$BelongsTo^2(x, X)$	element x belongs to set X

$$\varphi_{o4} = \forall i BelongsTo^2(i, \{1, 2, 3\}) \rightarrow \exists v (Eq^2(b_i^{(o)1}, v)) \quad (C.18)$$

$$\varphi_{o5} = \forall i BelongsTo^2(i, \{1, 2\}) \rightarrow \exists v (Eq^2(b_i^{(o)2}, v)) \quad (C.19)$$

- Activation Function Definition

$$\varphi_{o6} = \forall x (Eq^2(ReLU(x), \max(0, x))) \wedge \forall x (Eq^2(Identity(x), x)) \quad (C.20)$$

- Forward Propagation Rules

$$\begin{aligned} \varphi_{o7} = & \forall X \forall t (InputAt^2(X, t) \wedge BelongsTo^2(X, \mathbb{R}^2) \rightarrow \exists H (BelongsTo^2(H, \mathbb{R}^3) \\ & \wedge HiddenAt^2(H, t + \delta) \wedge \forall i (BelongsTo^2(i, \{1, 2, 3\}) \\ & \rightarrow Eq^2(h_i, ReLU \left(\sum_{j=1}^2 w_{ij}^{(o)1} \times x_j + b_i^{(o)1} \right)))) \end{aligned} \quad (C.21)$$

$$\begin{aligned} \varphi_{o8} = & \forall H \forall t (HiddenAt^2(H, t + \delta) \wedge BelongsTo^2(H, \mathbb{R}^3) \rightarrow \exists Y (BelongsTo^2(Y, \mathbb{R}^2) \\ & \wedge OutputAt^2(Y, t + 2\delta) \wedge \forall i (BelongsTo^2(i, \{1, 2\}) \\ & \rightarrow Eq^2 \left(y_i, Identity \left(\sum_{j=1}^3 w_{ij}^{(o)2} \times h_j + b_i^{(o)2} \right) \right))) \end{aligned} \quad (C.22)$$

- Backpropagation Rules

$$\begin{aligned}
 \varphi_{o_9} = & \forall X \forall Y_t \forall t (InputAt^3(X, Y_t, t) \wedge BelongsTo^2(Y_t, \mathbb{R}^2) \wedge \varphi_{o_7} \wedge \varphi_{o_8} \\
 & \wedge Eq^2(L, MSE(Y, Y_t)) \wedge Eq^2\left(MSE(Y, Y_t), \frac{1}{2} \sum_{i=1}^2 (y_i - y_{ti})^2\right)
 \end{aligned} \tag{C.23}$$

$$\begin{aligned}
 \varphi_{o_{10}} = & \varphi_{o_7} \wedge \varphi_{o_8} \wedge \varphi_{o_9} \\
 & \wedge Differentiable^2(MSE(Y, Y_t), W_1^{(o)}) \\
 & \wedge Differentiable^2(MSE(Y, Y_t), b_1^{(o)}) \\
 & \wedge Differentiable^2(MSE(Y, Y_t), W_2^{(o)}) \\
 & \wedge Differentiable^2(MSE(Y, Y_t), b_2^{(o)}) \\
 & \wedge Eq^2(\nabla_{W_1^{(o)}} L, \\
 & \quad ((W_2^{(o)})^T (Y - Y_t) \odot ReLU'(W_1^{(o)} X + b_1^{(o)})) X^T) \\
 & \wedge Eq^2(\nabla_{b_1^{(o)}} L, \\
 & \quad (W_2^{(o)})^T (Y - Y_t) \odot ReLU'(W_1^{(o)} X + b_1^{(o)})) \\
 & \wedge Eq^2(\nabla_{W_2^{(o)}} L, (Y - Y_t) (ReLU(W_1^{(o)} X + b_1^{(o)}))^T) \\
 & \wedge Eq^2(\nabla_{b_2^{(o)}} L, (Y - Y_t))
 \end{aligned} \tag{C.24}$$

- Learning Rules

$$\begin{aligned}
 \varphi_{o_{11}} = & \varphi_{o_7} \wedge \varphi_{o_8} \wedge \varphi_{o_9} \wedge \varphi_{o_{10}} \wedge Eq^2(W_1^{(u)}, W_1^{(o)} - \eta \nabla_{W_1^{(o)}} L) \\
 & \wedge Eq^2(b_1^{(u)}, b_1^{(o)} - \eta \nabla_{b_1^{(o)}} L) \wedge Eq^2(W_2^{(u)}, W_2^{(o)} - \eta \nabla_{W_2^{(o)}} L) \\
 & \wedge Eq^2(b_2^{(u)}, b_2^{(o)} - \eta \nabla_{b_2^{(o)}} L)
 \end{aligned} \tag{C.25}$$

In equation (A.14), the carrier M refers to the initially constructed model, and To_m denotes the time when model M is completed. Clearly, we have:

$$sup(To_h) \leq inf(To_m) \tag{C.26}$$

The state $S_M(M, To_m)$ is a one-to-one enabling mapping of the state $S_{oo}(oo, To_h)$ onto M , that is,

$$S_M(M, To_m) = \{\psi_{o_1}, \psi_{o_2}, \psi_{o_3}, \psi_{o_4}, \psi_{o_5}, \psi_{o_6}, \psi_{o_7}, \psi_{o_8}, \psi_{o_9}, \psi_{o_{10}}, \psi_{o_{11}}\} \tag{C.27}$$

and

$$Io(\varphi o_i) \supseteq \psi o_i (1 \leq i \leq 11) \quad (\text{C.28})$$

Here, the information Io enables the mapping from the initial ontological state of model M to its carrier state, that is, the initial state of M . In practice, this mapping is a complex process involving hardware implementation, software development, and hardware-software integration, inevitably requiring consumption of time and energy resources, and subject to various sources of noise. However, to simplify the discussion, we temporarily disregard these factors and explain the initial state of M using a completely ideal, noise-free, and recoverable information model. The subsequent discussions on other types of information will follow this approach and will not be repeated.

(2) Training Information of M

Based on MLT-MF, the training information for model M is as follows:

$$It = \langle ot, Tt_h, S_{ot}, Mt, Tt_m, S_{Mt} \rangle \quad (\text{C.29})$$

Here, the ontology ot refers to the object described by the training information, and the occurrence time Tt_h denotes the point at which this object attains its corresponding state attributes. The ontological state $S_{ot}(ot, Tt_h)$ represents the attributes of the object at time Tt_h , which are described by a set of well-formed formulas:

$$S_{ot}(ot, Tt_h) = \{\varphi t_1, \varphi t_2\} \quad (\text{C.30})$$

- Vector Definition

$$\varphi t_1 = \forall X \forall Y_t (\text{BelongsTo}^2(X, \mathbb{R}^2) \wedge \text{BelongsTo}^2(Y_t, \mathbb{R}^2)) \quad (\text{C.31})$$

- Label Consistency

$$\varphi t_2 = \forall X \forall Y_t \text{Eq}^2(\text{Target}(X), Y_t) \quad (\text{C.32})$$

The carrier Mt serves as the interface device through which model M receives training data, and Tt_m is the time at which model M is trained. The carrier state $S_{Mt}(Mt, Tt_m)$ is then described by the set of well-formed formulas:

$$It(\varphi t_i) \supseteq \psi t_i (1 \leq i \leq 2) \quad (\text{C.33})$$

(3) Optimized Information After M Has Learned from Training

Based on MLT-MF, after learning the training information It , model M updates its initial information Io to a new, optimized information state:

$$Iu = \langle ou, Tu_h, S_{ou}, M, Tu_m, S_M \rangle \quad (\text{C.34})$$

Here, the ontology ou is a fusion of M and the object described by the training information; the occurrence time Tu_h is the moment M learns from the training data; and the ontological state $S_{ou}(ou, Tu_h)$ represents the theoretical state of M after training:

$$S_{ou}(ou, Tu_h) = \{\varphi u_1, \varphi u_6, \varphi u_7, \varphi u_8, \varphi u_9, \varphi u_{10}, \varphi u_{11}\} \quad (\text{C.35})$$

Since the structure and algorithms of M remain unchanged before and after training, $\varphi u_1, \varphi u_6$, and φu_9 are exactly the same as $\varphi o_1, \varphi o_6$, and φo_9 respectively. Moreover, as the weights and biases after training are already assigned values in the original information (A.25), there is no need to include equivalent formulas for $\varphi o_2, \varphi o_3, \varphi o_4$, or φo_5 in $S_{ou}(ou, Tu_h)$. For the remaining formulas $\varphi u_7, \varphi u_8, \varphi u_{10}$, and φu_{11} , it suffices to systematically replace $W_k^{(o)}, w_{ij}^{(o)k}, b_k^{(o)}, b_i^{(o)k}, W_k^{(u)}, w_{ij}^{(u)k}, b_k^{(u)}$ and $b_i^{(u)k}$ in $\varphi o_7, \varphi o_8, \varphi o_{10}$, and φo_{11} with the corresponding symbols $W_k^{(u)}, w_{ij}^{(u)k}, b_k^{(u)}, b_i^{(u)k}, W_k^{(v)}, w_{ij}^{(v)k}, b_k^{(v)}$ and $b_i^{(v)k}$ in $S_{ou}(ou, Tu_h)$.

Similarly, the carrier state

$$S_M(M, Tu_m) = \{\psi u_1, \psi u_6, \psi u_7, \psi u_8, \psi u_9, \psi u_{10}, \psi u_{11}\} \quad (\text{C.36})$$

is a one-to-one enabling mapping from $S_{ou}(ou, Tu_h)$ onto M, representing the state of M after completing its training.

(4) Input Information for M

Processing input information is a fundamental requirement for any model. Based on the MLT-MF framework, the input information for M is defined as:

$$Iq = \langle oq, Tq_h, Soq, Mq, Tq_m, SMq \rangle \quad (\text{C.37})$$

Here, oq denotes the object described by the input information, and Tq_h is the time at which the object's state occurs. The state $Soq(oq, Tq_h)$ can take two possible forms:

- The first scenario involves only input information being processed by M, in which case

$$S_{oq}(oq, Tq_h) = \{\varphi q_1\} \quad (\text{C.38})$$

$$\varphi q_1 = \forall X \text{BelongsTo}^2(X, \mathbb{R}^2) \quad (\text{C.39})$$

- The second scenario considers online learning, where

$$S_{oq}(oq, Tq_h) = \{\varphi q_1, \varphi q_2\} \quad (\text{C.40})$$

$$\varphi q_1 = \forall X \forall Y_t (\text{BelongsTo}^2(X, \mathbb{R}^2) \wedge \text{BelongsTo}^2(Y_t, \mathbb{R}^2)) \quad (\text{C.41})$$

$$\varphi q_2 = \forall X \forall Y_t \text{Eq}^2(\text{Target}(X), Y_t) \quad (\text{C.42})$$

The carrier Mq for Iq serves as the input device for M, which may or may not be the same as the carrier Mt for the training information It . The state $S_{Mq}(Mq, Tq_m)$ is a one-to-one enabling mapping from $S_{oq}(oq, Tq_h)$ onto Mq .

(5) Information After M Processes Input, Produces Output, and Undergoes Further Optimization

There are two scenarios for M after it processes input and produces output: one corresponds to the first case in (4), where only output is produced without further optimization of the model itself; the other corresponds to the second case in (4), where, in the context of online learning, the model both produces output and undergoes further self-optimization. Since the latter is more comprehensive, we will focus on this scenario below.

In this case, the output information $I_r = \langle or, Tr_h, S_{or}, Mr, Tr_m, S_{Mr} \rangle$ has an ontological state defined as:

$$S_{or}(or, Tr_h) = \{\varphi_{r1}\} = \{\varphi_{o7} \wedge \varphi_{o8} \wedge OutputAt^2(Y, Tr_h)\} \quad (C.43)$$

The carrier state $S_{Mr}(Mr, Tr_m)$ is a one-to-one enabling mapping from $S_{or}(or, Tr_h)$ to the output device of M.

On the other hand, since we are considering the scenario where M performs online learning, the model now carries further optimized information:

$$I_v = \langle ov, Tv_h, S_{ov}, M, Tv_m, S_M \rangle \quad (C.44)$$

This structure is almost identical to the optimized information I_u after M has learned from training. The ontological state of I_v is:

$$S_{ov}(ov, Tv_h) = \{\varphi_{v1}, \varphi_{v6}, \varphi_{v7}, \varphi_{v8}, \varphi_{v9}, \varphi_{v10}, \varphi_{v11}\} \quad (C.45)$$

Here, φ_{v1} , φ_{v6} , and φ_{v9} are identical to φ_{u1} , φ_{u6} , and φ_{u9} respectively. For the remaining formulas, it suffices to systematically replace the parameters

$$W_k^{(u)}, w_{ij}^{(u)k}, b_k^{(u)}, b_i^{(u)k}, W_k^{(v)}, w_{ij}^{(v)k}, b_k^{(v)}, b_i^{(v)k}$$

in $S_{ou}(ou, Tu_h)$ with the corresponding parameters

$$W_k^{(v)}, w_{ij}^{(v)k}, b_k^{(v)}, b_i^{(v)k}, W_k^{(w)}, w_{ij}^{(w)k}, b_k^{(w)}, b_i^{(w)k}$$

to obtain the updated formulas, where $W_k^{(w)}$, $w_{ij}^{(w)k}$, $b_k^{(w)}$, and $b_i^{(w)k}$ are the weights and biases of M after further optimization.

Similarly, the carrier state

$$S_M(M, Tv_m) = \{\psi_{v1}, \psi_{v6}, \psi_{v7}, \psi_{v8}, \psi_{v9}, \psi_{v10}, \psi_{v11}\} \quad (C.46)$$

is a one-to-one enabling mapping from $S_{ov}(ov, Tv_h)$ onto M.

At this point, based on MLT-MF, we have constructed the formal well-formed formula representations for all ontological and carrier states of each component of the feedforward neural network model M, as illustrated in Fig. C.1. Although M is a simple model, it contains all the essential elements of a neural network, and the discussion has not relied on any special-case treatment of M. This demonstrates that MLT-MF is capable of supporting the construction of well-formed, formal representations for a wide variety of neural networks, providing a solid foundation for detailed analysis and optimization.